Quaternary Science Reviews 157 (2017) 80–97

Contents lists available at ScienceDirect

Quaternary Science Reviews

journal homepage: www.elsevier.com/locate/quascirev

Vegetation of Eurasia from the last glacial maximum to present: Key biogeographic patterns

Heather Binney [a], Mary Edwards [a, *], Marc Macias-Fauria [b], Anatoly Lozhkin [c], Patricia Anderson [d], Jed O. Kaplan [e], Andrei Andreev [f, g], Elena Bezrukova [h], Tatiana Blyakharchuk [i], Vlasta Jankovska [j], Irina Khazina [k], Sergey Krivonogov [l, m], Konstantin Kremenetski [n], Jo Nield [a], Elena Novenko [o], Natalya Ryabogina [p], Nadia Solovieva [q, r], Kathy Willis [b, 1], Valentina Zernitskaya [s]

[a] Geography and Environment, University of Southampton, Highfield, Southampton, SO17 1 BJ, UK
[b] School of Geography and the Environment, University of Oxford, South Parks Road, Oxford, OX1 3QY, UK
[c] North East Interdisciplinary Research Institute, Far East Branch, Russian Academy of Science, Magadan, 685000, Russia
[d] Quaternary Research Center, Box 351360, University of Washington, WA, 98195-1360, Seattle, USA
[e] Institute of Earth Surface Dynamics, University of Lausanne, CH-1015, Lausanne, Switzerland
[f] Institute of Geology and Mineralogy, University of Cologne, Zülpicher Str. 49a, D-50674, Cologne, Germany
[g] Institute of Geology and Petroleum Technologies, Kazan Federal University, Kremlyovskaya 18, 420008 Kazan, Russia
[h] Vinogradov Institute of Geochemistry, Siberian Branch of the Russian Academy of Sciences, 1A, Favorsky Str., Irkutsk, 664033, Russia
[i] Institute for Monitoring Climatic and Ecological Systems, Siberian Branch, Russian Academy of Sciences, Akademicheski Ave 10/3, 643055, Tomsk, Russia
[j] Institute of Botany, CAS, Zámek 1, 252 43, Průhonice, Czechia
[k] Petroleum Geology and Geophysics Siberian Branch of the Russian Academy of Sciences, Koptyuga Ave. 3, Novosibirsk 630090, Russia
[l] Sobolev Institute of Geology and Mineralogy SB RAS, Koptyuga Ave. 3, Novosibirsk, 630090, Russia
[m] Novosibirsk State University, Pirogova St. 2, Novosibirsk, 630090, Russia
[n] Department of Geography, University of California-Los Angeles, Los Angeles, CA, 90095-1524, USA
[o] Faculty of Geography, Lomonosov Moscow State University, Moscow, Russia
[p] Institute of Problems of Development of the North, Siberian Branch of the Russian Academy of Sciences, Russia
[q] Environmental Change Research Centre, University College London, Gower Street, London, WC1E 6BT, UK
[r] Higher Colleges of Technologies, University City, Sharjah, PO Box 7947, United Arab Emirates
[s] Institute of Natural Management, NAS of Belarus, F. Skorynu Str. 10, 220114, Minsk, Belarus

ARTICLE INFO

Article history:
Received 26 July 2016
Received in revised form
14 November 2016
Accepted 15 November 2016
Available online 27 December 2016

Keywords:
Eurasia
Pollen
Biomes
Vegetation
Late Quaternary

ABSTRACT

Continental-scale estimates of vegetation cover, including land-surface properties and biogeographic trends, reflect the response of plant species to climate change over the past millennia. These estimates can help assess the effectiveness of simulations of climate change using forward and inverse modelling approaches. With the advent of transient and contiguous time-slice palaeoclimate simulations, vegetation datasets with similar temporal qualities are desirable. We collated fossil pollen records for the period 21,000–0 cal yr BP (kyr cal BP; calibrated ages) for Europe and Asia north of 40°N, using extant databases and new data; we filtered records for adequate dating and sorted the nomenclature to conform to a consistent yet extensive taxon list. From this database we extracted pollen spectra representing 1000-year time-slices from 21 kyr cal BP to present and used the biomization approach to define the most likely vegetation biome represented. Biomes were mapped for the 22 time slices, and key plant functional types (PFTs, the constituents of the biomes) were tracked though time. An error matrix and index of topographic complexity clearly showed that the accuracy of pollen-based biome assignments (when compared with modern vegetation) was negatively correlated with topographic complexity, but modern vegetation was nevertheless effectively mapped by the pollen, despite moderate levels of misclassification for most biomes. The pattern at 21 ka is of herb-dominated biomes across the whole region. From the onset of deglaciation (17–18 kyr cal BP), some sites in Europe record forest biomes, particularly the south, and the proportion of forest biomes gradually increases with time through 14 kyr cal BP. During the same period, forest biomes and steppe or tundra biomes are intermixed across

* Corresponding author.
E-mail address: m.e.edwards@soton.ac.uk (M. Edwards).
[1] Present address: Department of Zoology, University of Oxford, South Parks Road, Oxford, OX1 3PS, UK.

http://dx.doi.org/10.1016/j.quascirev.2016.11.022

the central Asian mountains, and forest biomes occur in coastal Pacific areas. These forest biome occurrences, plus a record of dated plant macrofossils, indicate that some tree populations existed in southern and Eastern Europe and central and far-eastern Eurasia. PFT composition of the herbaceous biomes emphasises the significant contribution of diverse forbs to treeless vegetation, a feature often obscured in pollen records. An increase in moisture ca. 14 kyr cal BP is suggested by a shift to woody biomes and an increase in sites recording initialization and development of lakes and peat deposits, particularly in the European portion of the region. Deforestation of Western Europe, presumably related to agricultural expansion, is clearly visible in the most recent two millennia.

1. Introduction

Northern Eurasia (north of ca. 40°N and from 10°W to 180°E) is a large landmass with distinct gradients in climate. The last deglaciation led to dramatic changes to the Earth system, and in the North polar amplification likely enhanced regional responses to climate forcing (Serreze and Barry, 2011). The geography of Eurasia altered dramatically as the extensive shallow coastal shelves bordering the Arctic Ocean and the shallow Bering Strait region, which were subaerial for much of the last glacial-interglacial cycle, were flooded by eustatic sea-level rise. The biotic system saw major shifts in vegetation structure and composition (Andreev and Tarasov, 2013; Lozhkin and Anderson, 2013; Willerslev et al., 2014), continental-scale ecotones between forest and steppe and forest and tundra being particularly sensitive recorders of climate change (e.g., Pielke and Vidale, 1995; Thompson et al., 2004; Williams et al., 2011). Changes in the size of mammalian populations and local and global extinctions occurred (Sher, 1997; Stuart et al., 2004; Barnosky et al., 2004). There were changes in the terrestrial carbon sink, such as the development of peatlands (Smith et al., 2004), in patterns of thermokarst and permafrost degradation (Zimov et al., 2006; Walter et al., 2007) and in other nutrient cycles (McLauchlan et al., 2013). To date, the late-Quaternary changes in Eurasian vegetation have not been comprehensively summarized and mapped using palaeodata.

How well key climate changes are depicted in palaeoclimate simulations can be examined via comparison with spatio-temporal vegetation changes on a large scale. Recent climate simulations have used contiguous time-steps over long periods (i.e., independent simulations for a set of time-slices; Singarayer and Valdes, 2010), or transient runs (i.e., continuous simulation over a given time span; e.g., Liu et al., 2009). Several comparisons have been made for the last glacial maximum (LGM), 6 kyr cal BP and present (e.g., Kaplan et al., 2003; Wohlfahrt et al., 2008; Bartlein et al., 2011), and Hoogakker et al. (2016) examined snapshots of compiled environmental data through the last glacial cycle with simulated data. To be effective, this type of exercise requires suitable comparator datasets. Pollen data remain by far the most abundant and widespread source of information about late-Quaternary vegetation change. Compared with other regions, the Siberian sector is described by relatively sparse palaeodata, but more pollen data are becoming available and can be compared with information from other sources, e.g. plant macrofossils (Binney et al., 2009) or ancient DNA (Willerslev et al., 2014). Here we build on the efforts of the PAIN project (e.g., circumpolar vegetation reconstructions for 6ka and 21 ka: the Pan-Arctic INitative; Bigelow et al., 2003) plus new data synthesized in an international workshop to develop a series of pollen-based biome reconstructions from 21 to 0 kyr cal BP for Eurasia north of 40°N. We used dated pollen records from geo-archives to map vegetation biomes using the biomization algorithm of Prentice et al. (1996) modified by Bigelow et al. (2003). We present time-slice maps of biomes and describe the most prominent changes, assess uncertainty in the biome assignments, and discuss the key emergent patterns in relation to changing Quaternary climates, distribution changes of key plant taxa and the sustainability of the Eurasian megafauna. We also summarize the dynamics of major plant functional types (PFTs) as they relate to key land-cover properties.

2. Study area

The study region extends from the Iberian Peninsula to easternmost Siberia north of 40°N (Fig. 1). In our results and discussion we distinguish eastern and western sectors delineated by the 40° E meridian. West of ca. 40°E lies largely mountainous Europe; to the east are the extensive Russian and western Siberian plains. A series of broad lowlands characterize the region east of the Taimyr Peninsula into northeast Siberia. These lowlands are bordered by a series of north-south mountain complexes. The southern fringe of the study region is marked by the Mediterranean Sea in the west and central Asian mountain ranges and basins further east. Potential current natural vegetation includes temperate and mixed forests, boreal forest, temperate grassland (steppe) and alpine and arctic tundra (Fig. 2). West of 40°E in particular, extensive forested regions have been transformed by agriculture.

Considerable climatic variation is reflected in the range of modern biomes that characterize the continent (Fig. 2). A latitudinal maritime-continental gradient is evident: steppe and desert regions occupy the arid continental interior south of ~50°N, while the presence of Atlantic and Pacific Oceans in the west and east, respectively, is linked to temperate conditions and deciduous or mixed-deciduous forest cover. In Europe, the southern margins of the study region feature a Mediterranean climate and evergreen sclerophyll vegetation. Mean annual precipitation across the boreal forest zone (north of ~50°N) ranges from over 1000 mm in mountainous Scandinavia to ~200 mm in northeast Siberia; evergreen coniferous forest in the western part of the continent grades to deciduous coniferous forest in the east. Annual temperature ranges in the eastern boreal region can be > 60 °C. The northern edge of the landmass and higher elevations support tundra, with cool growing season means below 10 °C and cold winters.

During the cold, dry glacial maximum centred on 21 kyr cal BP glaciation was relatively restricted compared with earlier phases of the last glacial cycle. Ice covered Scandinavia and adjacent areas but barely affected the western and central Siberian lowlands (Svendsen et al., 2004). In northeast Siberia (here defined as lands lying east of the Verkhoyansk Range), glaciation was largely restricted to the mountains (Barr and Clark, 2012; Velichko and Faustova, 2009). Thus much of the study region remained unglaciated between the LGM and present.

Palaeoecological records of full-glacial age from across the region from the Atlantic to the Pacific have long been interpreted as representing treeless vegetation that supported a diverse grazing megafauna (Guthrie, 1990) and small bands of human hunter-

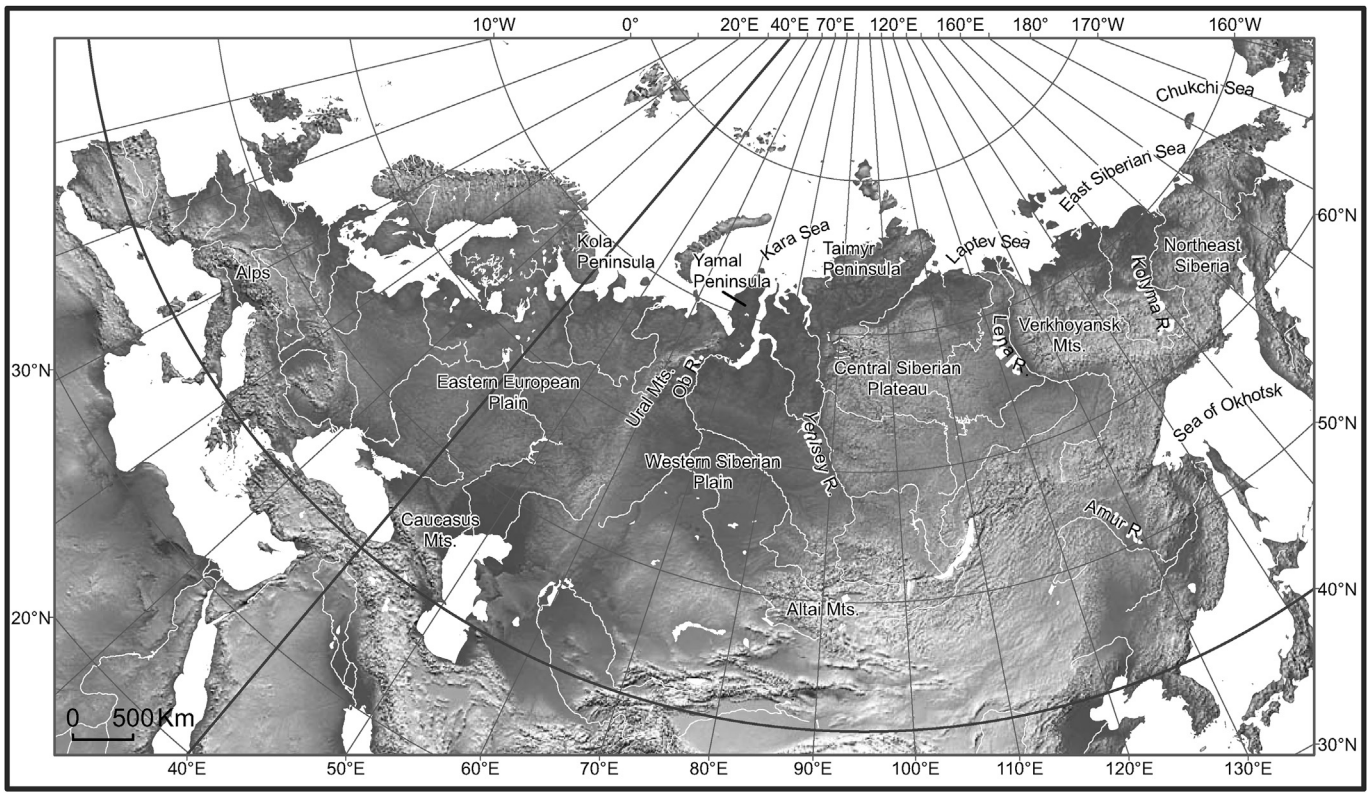

Fig. 1. Map of study area showing topography and geographic features named in the text. The southern limit of the study area is 40°N (designated by a thicker line). The 40°E meridian is also emphasized. This marks the break between the "western" and "eastern" portions of the study area used in various analyses.

gatherers (Pitulko et al., 2004). However, growing evidence points to persistence of boreal and temperate tree taxa across the region in a variety of refugia (Stewart and Lister, 2001; Birks and Willis, 2008; Binney et al., 2009; Huntley et al., 2013). Subsequent vegetation changes are likely linked with the demise of much of the grazing megafauna (with the direction of causality still contested; Zimov et al., 1995; Stuart et al., 2004; Zimov, 2005; Campos et al., 2010). Deglaciation was marked by climate oscillations, most notably the Younger Dryas (12.9–11.7 ka; Rasmussen et al., 2006 and Lowe et al., 2008), although this feature is not recorded across the whole study region. With a shift to warmer and moister interglacial climates, treeless vegetation was replaced by boreal or temperate forest over much of the region, and wetland extent increased (Lozhkin et al., 2011; Andreev and Tarasov, 2013). Recent millennia have seen human transformation of vegetation cover, particularly in Europe (e.g., Gaillard et al., 2008; Kaplan et al., 2009; Trondman et al., 2015; Fyfe et al., 2015).

3. Methods

Biomization of pollen data is the process whereby inferred vegetation can be represented by a relatively small number of biomes that describe major structural, functional and floristic differences. Key to the process is preparation of a high-quality database, which requires considerable checking of data and metadata and decisions about site chronologies, taxonomy and biomization rules. The Supplementary On-line Material (SOM) contains details of methodological approaches. Below are brief descriptions of the main features of the sites, samples used, and key decisions made in database construction and biomization.

3.1. Data sources

The pollen database used in this study was constructed by the authors from several sources, including extant public databases and previously unpublished data. Because of geographic differences in site densities, we present results both across the total study area and separately for Europe and adjacent Asia. Table S1 in the Supplementary Online Material (SOM) provides basic metadata for the biomized samples and accompanying text describes quality control decisions. The total number of sites is 5858, the majority of which are modern surface/core-top samples (Fig. 3). Data from more than one discrete section from the same (terrestrial) exposure were amalgamated to form one site.

3.2. Chronologies

All sites had their own radiocarbon chronologies (i.e., no sites were dated by correlation). We used previously generated, calibrated chronologies when available. For new, uncalibrated chronologies or chronologies that used conventional radiocarbon ages, we used CLAM v. 1.2 (Blaauw, 2010) to calibrate dates and construct new age models. For extant age models in ^{14}C years, we converted ages using the "quick calibration curve" (NEOTOMA, Eric Grimm, http://www.neotomadb.org/, based upon the INTCAL04 calibration curve of Reimer et al., 2004). Fig. 3 shows the temporal distribution of samples, which were classified in to age slices. We used pollen values of the sample closest to the midpoint of the 1000-yr calibrated age slice. To avoid samples falling into more than one age slice, samples were omitted when the reported error on the age calibration/age model was >500 yr, except for 21 kyr cal BP, for which we experimented with both a 500-yr and a 1000-yr limit. All ages are given in calibrated years

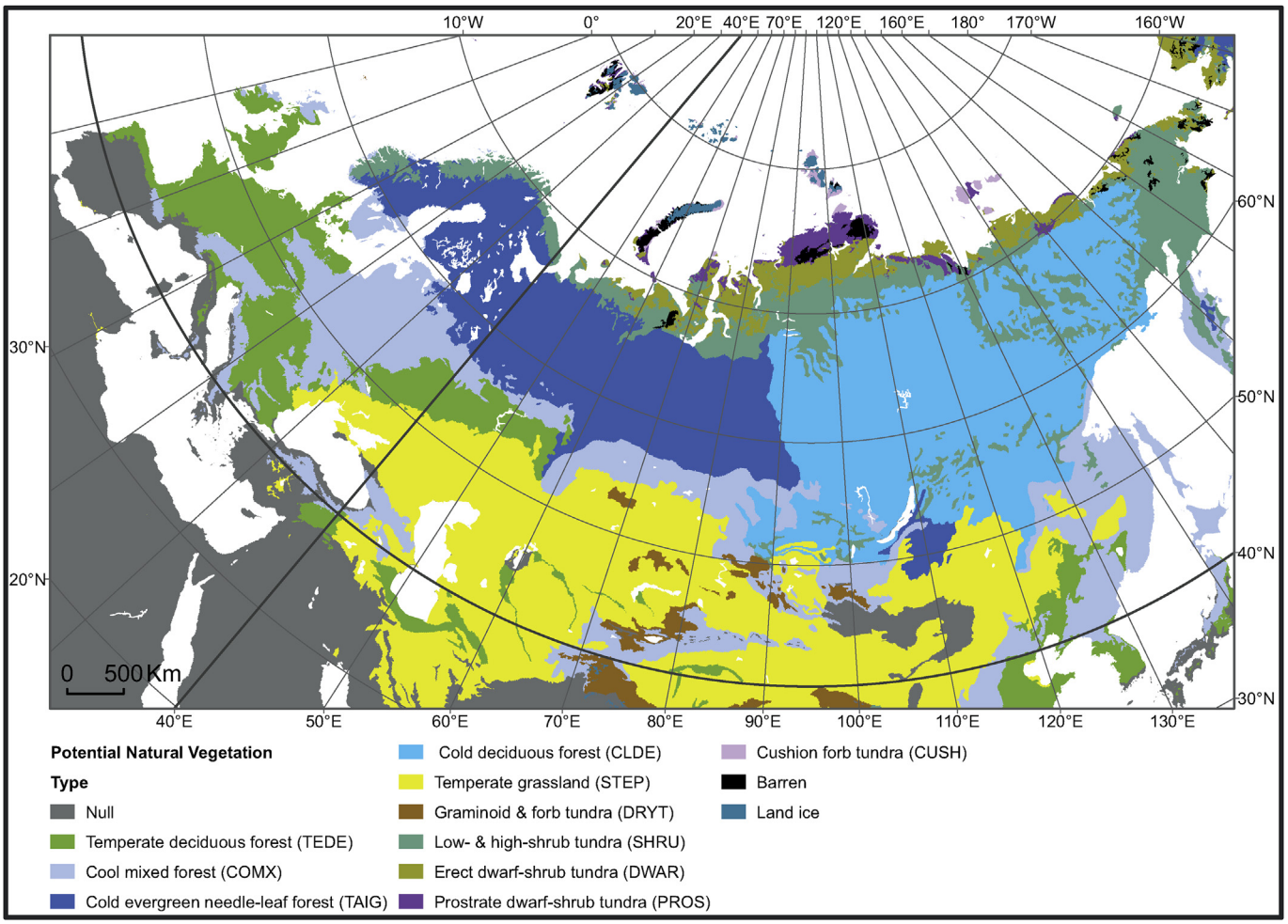

Fig. 2. Potential natural vegetation of the study area; 40°N and 40°E lines are emphasized. The null designation is used beyond the study area, except where at 40°N the continuity of a biome southward is clarified by extending its polygon. Null is used within the study region to represent desert in south-central Asia and Mediterranean sclerophyll forest (note: the latter is not included in the analyses).

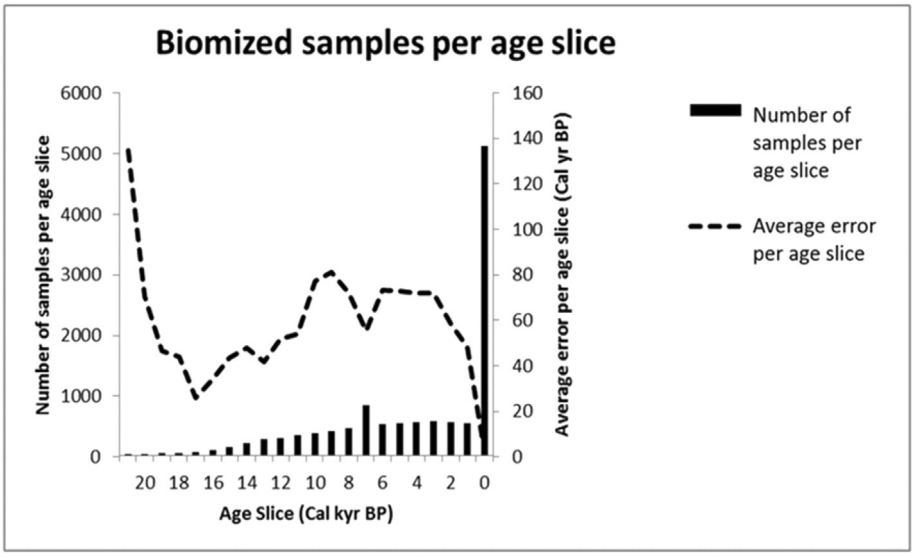

Fig. 3. The number of samples assigned to each age class and the average reported error per time slice.

before present, depicted by kyr BP in the following sections.

3.3. Taxonomy and choice of biomes

Great care was taken to produce a dataset with a consistent taxonomy. The checked, redundancy-free taxonomy includes 2874 taxa. We incorporated a diversity of minor herb types attributable to open-land biomes. Potential natural vegetation is used to estimate the effectiveness of modern biomization patterns in the northern extra-tropics because tree pollen dominates modern spectra, even in predominantly agricultural areas, and previous evaluations of modern vegetation-pollen patterns have shown a relatively good match (Prentice and Webb, 1998). While several maps of Eurasian potential natural vegetation exist, none has the appropriate resolution of vegetation categories for comparison with our biomized data. We therefore created a map specifically to assess the distribution of pollen-based biomes against modern vegetation (see SOM for more details). We excluded the Mediterranean sclerophyll biome. While occurring today within the study area boundaries, it was more restricted in the past, and only a few sites are affected by its removal.

The map of potential natural vegetation displays polygons that all relate to the biomes used in the biomization (Fig. 2, Table 1). We used a restricted distribution of desert, as desert sites typically classify as steppe pollen biomes. We collapsed the cool-temperate evergreen needle-leaved forest biome into the cool mixed forest because the groups of constituent taxa for both biomes in northern Eurasia are almost identical. Inclusion of both introduced unnecessary noise into biome assignments while adding little extra information on land-cover change.

3.4. Biomization

The BIOME 6000 approach to synthesizing pollen data into vegetation biomes (Prentice and Webb, 1998) focuses on the contribution of plant-functional types (PFTs) to the total pollen sum, using fuzzy logic to calculate the most probable dominant biome. It is therefore not species-dependent. The known biases of pollen representation are moderated using a simple square-root transformation. Binney et al. (2011) showed that this simple function performs moderately well in balancing the relative overproduction of most boreal tree/shrub taxa against the underrepresentation of most forbs. The pollen biomes used are a subset of those simulated by BIOME 4 (Kaplan et al., 2002). This means our dataset has the potential for direct comparison with palaeovegetation simulations. We follow the biomization approach used by Bigelow et al. (2003), except we added desert (DESE; see Table 1) and collapsed two mixed forest biomes (see Section 3.2 above).

We defined 30 PFTs (see Table 2). A total of 752 taxa were used in biomizations; the remainder were omitted because they only occurred once or twice, or because they were taxonomically or ecologically ambiguous. The taxon-PFT table (Table S2) and the PFT-Biome (Table S3) are presented in the online supporting material. We used a biomization program written in Matlab and described in Binney et al. (2011).

The biomes are primarily presented as biome "dotmaps". Each site with a sample in the age slice of interest is mapped according to a colour-coded key. Where dots overlap, we chose to map the biomes giving preference to open-land biomes, which resulted in a visual bias towards this biome type.

Following Bigelow et al. (2003), the *Larix* pollen values were multiplied by a factor of $\times$15 prior to biomization, because of the importance of the taxon across Siberia and its exceedingly low level of representation in pollen spectra. For NE Siberia (E of the Verkhoyansk Ranges, ca. >155° E) we made the assumption that *Pinus* pollen (sub-genus Haploxylon) derived from *P. pumila*, the only taxon in the region today. Percentages for all taxa were calculated using the total terrestrial pollen sum, and a square-root transformation of the pollen percentages was applied prior to biomization (Prentice and Webb, 1998; Binney et al., 2011).

A slightly different biomization scheme has been applied to the northern high latitudes in previous work by Tarasov et al. (1998, 2000, 2013). Tundra remains one biome, rather than being subdivided, and *Larix* is given a multiplier of $\times$20. A visual comparison of biome results suggests the latter is an inconsequential difference. However, because there is no dry tundra category (DRYT) in the Tarasov et al. studies, the constituent taxa for steppe (STEP) differ significantly between the two systems. For the LGM, particularly in the northern portion of the study area, our biomization procedure typically registers DRYT where Tarasov et al. (2000) register STEP. The nature of the zonal vegetation of the LGM (dry, cool conditions) was addressed by Kaplan et al. (2003), who described a bioclimatic envelope drier than most contemporary tundra and cooler than steppe. In much palaeoecological literature, this vegetation has been described as "steppe-tundra" or "tundra-steppe" (see Anderson et al., 2004; Andreev and Tarasov, 2013; Lozhkin and Anderson, 2013). Samples from site records unavailable to us but biomized by Tarasov et al. (2000) are plotted for 21,000 yr BP (see section 4.3 below).

3.5. Super PFTs

Summaries of structural-functional changes in land cover were created by defining "super PFTs" (unique groupings of PFTs in broad types, such as woody deciduous and graminoids) and calculating sums for each time slice for the eastern and western sectors of the study area. No taxon occurred in more than one super PFT. Using the biomization taxon-PFT look-up table, we summed scores for the following groups: grasses, sedges, forbs (excluding *Artemisia*), *Artemisia*, Ericales, *Sphagnum*, woody angiosperms and gymnosperms. *Artemisia* is in its own PFT because it represents shrub as well as forb taxa, particularly in STEP, and it has high pollen representation. The super-PFT values were summed for each age slice and a super-PFT sum created, which was used to calculate a percentage value for each super-PFT. Additionally, summed percent values of i) woody biomes and ii) non-woody biomes were calculated separately for areas to the west and east of 40°E for 500-yr time-slices before, during and after the Younger Dryas stade (YD, i.e., 13,500 to 10,500 kyr cal BP). This separation allows temporal patterns across the majority of the northern Eurasian land mass to be assessed without being masked by the large number of European sites (see Fig. 4a and b).

Table 1
Biomes used in the analysis.

Biome code	Biome name
DESE	desert
CUSH	cushion-forb tundra
DRYT	dry tundra: graminoids and forbs
PROS	prostrate dwarf-shrub tundra
DWAR	erect dwarf-shrub tundra
SHRU	low- and high-shrub tundra
STEP	temperate grassland
CLDE	cold deciduous forest
TAIG	cold evergreen needle-leaved forest
COCO	cool evergreen needle-leaved forest
TEDE	temperate deciduous forest
COMX	cool mixed forest

Table 2
Plant functional types used in the biomization.

Plant functional types
Bog moss (*Sphagnum*)
Grass graminoid
Sedge graminoid
Rush graminoid
Rosette or cushion forb
Arctic forb
Boreal or temperate drought-tolerant forb
Arctic cold-deciduous malacophyll broad-leaved prostrate dwarf shrub
Arctic evergreen malacophyll broad-leaved prostrate dwarf shrub
Arcto-boreal evergreen needle-leaved prostrate dwarf shrub
Arcto-boreal cold-deciduous malacophyll broad-leaved erect dwarf shrub
Arcto-boreal evergreen malacophyll broad-leaved erect dwarf shrub
Arcto-boreal cold-deciduous malacophyll broad-leaved low or high shrub
Arcto-boreal evergreen malacophyll broad-leaved low or high shrub
Arcto-boreal evergreen needle-leaved low or high shrub
Boreal cold-deciduous malacophyll broad-leaved low or high shrub
Boreal evergreen malacophyll broad-leaved low or high shrub
Boreal or temperate drought-tolerant cold-deciduous or evergreen malacophyll broad-leaved low or high shrub
Boreal evergreen needle-leaved tree
Boreal cold-deciduous needle-leaved tree
Boreal cold-deciduous malacophyll broad-leaved tree
Eurythermic evergreen needle-leaved tree
Temperate evergreen needle-leaved tree
Maritime evergreen needle-leaved tree
Cool-temperate evergreen needle-leaved tree
Temperate (spring-frost avoiding) cold-deciduous malacophyll broad-leaved tree
Temperate (spring-frost tolerant) cold-deciduous malacophyll broad-leaved tree
Temperate (spring-frost intolerant) cold-deciduous malacophyll broad-leaved tree
Temperate evergreen malacophyll broad-leaved woody plants
Desert forb/shrub

3.6. Macrofossils

In certain situations, pollen values do not clearly portray important aspects of the vegetation. For example, *Larix* poses a problem to all pollen-based reconstructions because of the extremely low pollen representation (see above). Small (possibly refugial) populations of various tree species may also be virtually undetectable in the pollen record (Stewart and Lister, 2001; Birks and Willis, 2008). Records for key woody taxa from the New Eurasian Macrofossil Database (NEMDB; Binney et al., 2009; http://oxlel.zoo.ox.ac.uk/resources/) enhance the relatively sparse pollen data coverage during the last glacial maximum (time slices 21–18 kyr cal BP) and help delimit northern treeline. The database contains numerous records of woody taxa at (and beyond) modern treeline, including *Larix, Pinus*, and *Picea*.

3.7. Modern pollen-vegetation analysis

Pollen sites are point data while mapped vegetation is in the form of raster data, and point-to-pixel comparisons are not the most effective way to assess how well mapped vegetation and pollen-based biomes match. Pollen sites integrate vegetation on a range of spatial scales (Bigelow et al., 2003; Sugita, 2007a,b) and thus the relevant size of a 'point' varies from site to site. Furthermore, vegetation representation by pollen is affected by other scaling factors. For example, where there is relatively flat topography (and relatively homogenous vegetation) pollen-based data usually match regional vegetation well. In mountainous regions there is a complex vegetation mosaic, the pollen signal is mixed, and the probability that at any one pollen site/grid cell will match the vegetation is lower. Northern Eurasia offers the opportunity to evaluate this effect as it has both extensive plains and mountain complexes, a factor which we incorporated into our assessment of the effectiveness of modern pollen biomization.

We compared modern biome identifications with mapped vegetation using an error matrix approach. To test the influence of topography on biomization effectiveness, we created a ruggedness index for all 100 × 100-km cells over Eurasia, using an elevation model at 1-km resolution. The ruggedness index reflects the sum of the slopes of every 1-km cell within each 100 × 100 km cell. The larger the slope sum, the more rugged is the terrain. Then we computed, for each pollen site, whether the vegetation map grid cell identity and the biomization result matched (0 = error, 1 = match). All positive matches and all errors were grouped separately and tested for difference in ruggedness using a *t*-test for two samples of unequal variance (the latter tested with an F-test).

4. Results

4.1. Modern pollen biomes compared with modern vegetation

A qualitative visual inspection of the biomized modern sample dataset overlain on potential natural vegetation shows good matches between pollen biomes and vegetation across Siberia, central Asia and northern Europe (Fig. 4a). Evergreen boreal forest (TAIG), cold deciduous forest (CLDE), cool mixed forest (COMX) and steppe (STEP) are delineated by a dominance of matching biome points but also include a scatter of other biome types. The four tundra biomes that occur along the Arctic coast and on high-arctic islands are moderately well reproduced by the pollen (Fig. 4a). Dry tundra (DRYT) is virtually absent in modern tundra vegetation in this region but is mapped in high-elevation areas of central Asia.

In western and central Europe (Fig. 4b), the boreal forest zone is clearly demarcated by the pollen. Mountainous regions are dominated by a mixture of temperate deciduous (TEDE) and cool mixed forest (COMX) biomes, with the latter predominant at the boreal-nemoral ecotone. Cool conifer forest (COCO) is not mapped as an extant vegetation biome (Fig. 2), but some pollen sites are classified

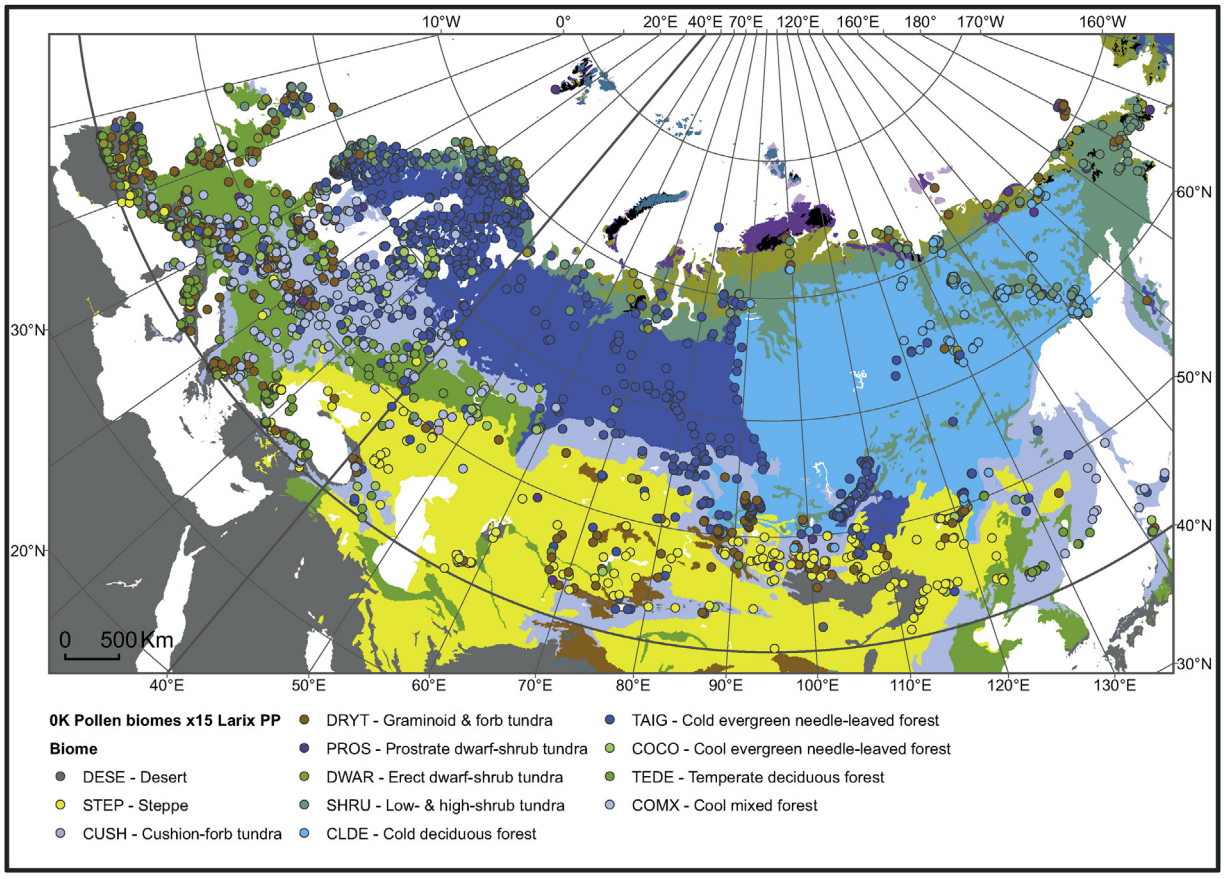

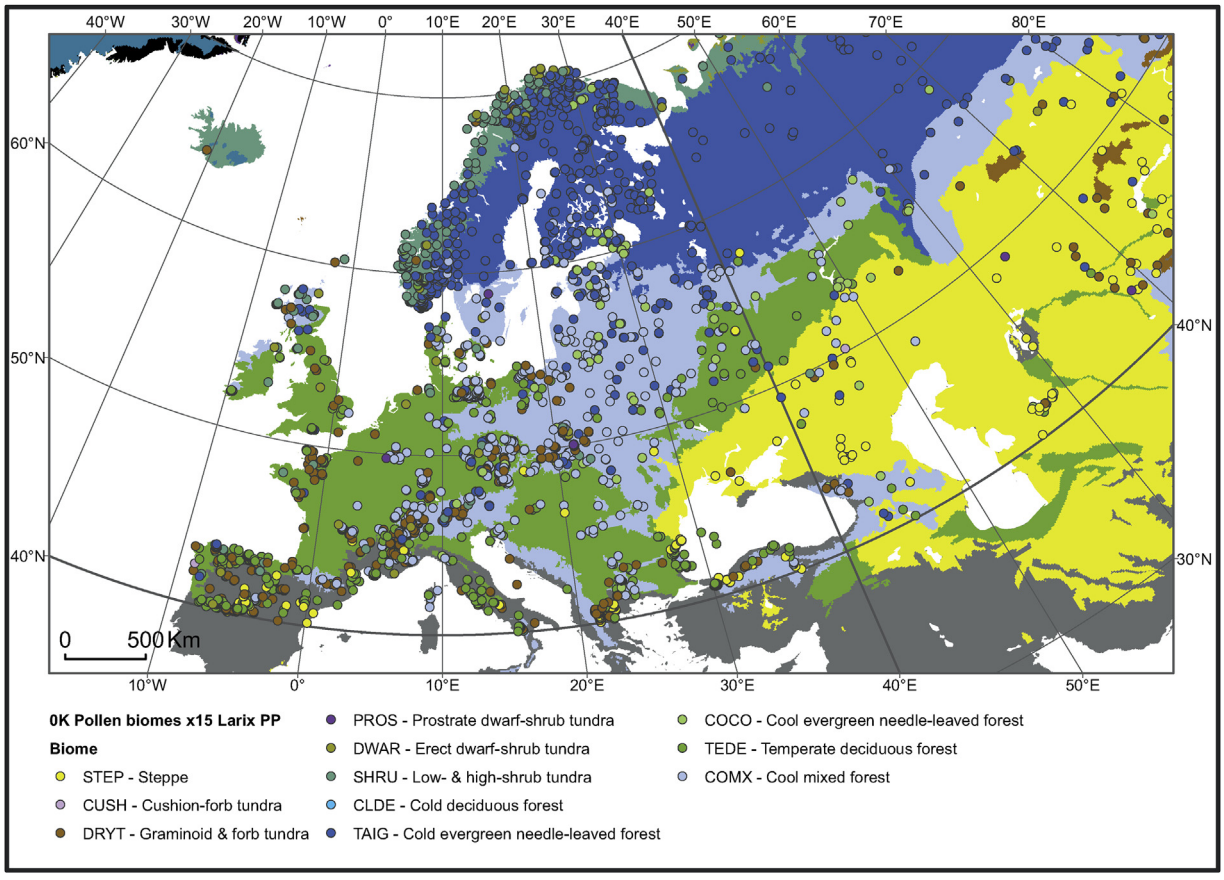

Fig. 4. a. Modern pollen biomes superimposed on potential natural vegetation map for Eurasia. The key is as before. The one site biomized as desert is shown with the null colour. b. Modern pollen biomes superimposed on potential natural vegetation map for Europe, at a more detailed scale than Fig. 4a.

as COCO. Steppe (STEP) is identified at sites east of the Black Sea. It is notable that the open-land biome dry tundra (DRYT) is common across the northern European lowlands, the British Isles and the northern Iberian Peninsula, where the potential natural vegetation would be forest but the majority of land is currently used for agricultural production.

While any vegetation map on this broad scale inevitably simplifies ecotonal boundaries and within-biome heterogeneity, the mapped locations of major biomes and their ecotones are well matched by the pollen: steppe-forest in southern Siberia and central Asia, the boreal-deciduous forest in Europe and western Asia, and the longitudinal ecotone between the two coniferous biomes in Siberia.

A numerical table of the results of the error analysis (Table S4, Table 3) quantifies i) the success with which a given pollen biome predicted its mapped biome and ii) for a given mapped biome, the rate at which it was successfully predicted by pollen. The critical patterns are discernible in the mapped data upon close inspection. For example, the mapped distribution of cold evergreen needle-leaved forest (TAIG) is well identified by pollen (84% of mapped points in this biome are TAIG). However, pollen records classified as TAIG are often in error, having a success rate of only 34% (i.e. many TAIG points fall into other biome polygons). Cool mixed forest (COMX) and temperate deciduous forest (TEDE) biomized points predicted the location of the mapped biomes with moderate success (43 and 41%, respectively). Here, much of the error can be explained by a reciprocal relationship (i.e., TEDE polygons are frequently characterized by COMX pollen biome points, and COMX polygons by TEDE points). These two biomes are physiognomically similar in their constituent taxa. Non-forest biomes are not well defined quantitatively because non-forest regions receive tree pollen from forested regions, which can cause pollen spectra to be biomized as forest biomes (see section 3.3. above). Furthermore, extremely poor relationships may be partly a function of few pollen points and/or small vegetation areas.

The relationship of landscape ruggedness with biomization success was strongly significant ($p = 4.86\ e^{-13}$). A logistic regression on the binary data (1, Match, 0, error), showed that the variable *ruggedness* (slope sum) is a predictor of biomization success ($p = 7.20\ e^{-12}$).

4.2. Temporal coverage

As radiocarbon errors tend to increase with age of sediment (Fig. 3) and older sites tend to be sampled at low temporal resolution, several possible samples were excluded from older time-slices. This, together with the fact that old sites are rare, means that prior to 14 kyr cal BP, site coverage is sparse, particularly in Siberia. The 21-ka time slice, however, features a larger dataset as 21 kyr cal BP is a critical time slice for comparison with simulations derived from climate modelling. For this time slice we relaxed the error limit, which added several more sites (for all sites see Fig. S1, 21 kyr cal BP).

Table 3
Error analysis for the spatial comparison between vegetation and pollen biomes. The middle column indicates the percent success of a given pollen-derived biome at falling within its vegetation region. The right-hand column shows the percentages of points within a given biome type that are correctly identified by the biomized pollen. The main features underlying the observed errors are also given.

Biome	Biomize: success at prediction	Vegetation biome assignments
Temperate deciduous forest (TEDE)	41% correct; most errors were where sites are in cold mixed forest, particularly in the Balkans, the Pyrenees, Turkey, and the Alps.	19% correct; other sites are biomized as COMX (44%, mostly in Central and Eastern Europe) and dry tundra (DRYT, 19%, mostly in Western Europe, but also in Inner Mongolia in China).
Cool mixed forest (COMX)	43% correct; errors show a reciprocal pattern with TEDE (see above), with sites displaying this error scatted across much of the biome's range, except in Western Europe, where it is rare.	29% correct; other sites are biomized as DRYT (22%, Pyrenees, Alps, Balkans, Pontic, Caucasus, Mongolia, north-central Europe), TEDE (19%, mostly in Western and Central Europe), and evergreen boreal forest (TAIG, 17%, in locations adjacent to the ecotone between TAIG and COMX).
Evergreen boreal forest (TAIG)	34% correct; TAIG also tends to be attributed to sites located in COMX (22%), cold deciduous forest (CLDE, 17%), and low-high shrub tundra (SHRU, 15%). TAIG is generally over-estimated by biomization.	84% correct; other sites tend to be biomized as COMX (13%, mostly in Finland).
Cold deciduous forest (CLDE)	69% correct; CLDE also tends to be attributed to sites in SHRU (16%) at the forest-tundra ecotone and in northern mountainous areas.	32% correct; other sites tend to be biomized as TAIG (38%) and SHRU (21%, largely in the far east of the region).
Temperate grassland or steppe (STEP)	41% correct; also tends to be attributed to sites in COMX (22%, mainly in European and central Asian mountain areas), TEDE (20%, in central France, Eastern China and Black Sea region) and desert (DESE; 12%, Central Asia).	40% correct; other sites tend to be biomized as DRYT (27%, mostly in Inner Mongolia and easternmost China) and TAIG (10%, Central Asia and Eastern Europe).
Desert (DESE)	0% correct; only one sample, which was mapped on to STEP	0% correct; DESE sites were biomized as STEP (63%, all over the biome range), DRYT (17%, Central Asia), and COMX (10%, Europe, Caspian and Aral Seas).
Dry tundra (DRYT)	6% correct; tends to be attributed to sites in COMX (45%) and TEDE (29%) across much of western and central Europe and Mongolia, and STEP (10%, Central Asia).	56% correct; other sites tend to be biomized as TAIG (23%, Altai Mountains and northern regions) and STEP (14%).
Low-high shrub tundra (SHRU)	38% correct; tends to be attributed to sites in CLDE (24%, mountainous Russian Far East), COMX (15%, Scotland, Alps, SW Norway) DWAR (10%, eastern Eurasian tundra).	35% correct; other sites tend to be biomized as TAIG (36%, Western Eurasia) and DWAR (11%, Norway).
Dwarf-shrub tundra (DWAR)	10% correct; tends to be attributed to sites in SHRU (37%, Norwegian mountains), COMX (21%, Alps, Pyrenees, Central Asian mountains), and TEDE (19%, Western Europe).	15% correct; other sites tend to be biomized as SHRU (47%, all over), PROS (15%, eastern Siberia), and DRYT (12%, widespread).
Prostrate −shrub tundra (PROS)	0% correct; tends to be attributed to sites in DWAR (31%, NE Eurasian tundra), COMX (19%, mountains), STEP (19%), TEDE (10%, Asia), and CLDE (10%).	0% correct; other sites tend to be biomized as SHRU (89%), and CLDE (11%); mostly lower Lena River.
Cushion-forb tundra (CUSH)	0% correct; tends to be attributed to sites in TEDE (30%, Western European mountains), STEP (23%, Eastern China), CLDE (20%, near treeline), and COMX (17%, Western Europe)	No sites
Barren (BARR)	No sites were biomized as barren.	0% correct; other sites tend to be biomized as DRYT (55%, Taiymyr) and SHRU (36%, Chukotka)

4.3. Past vegetation biomes for Eurasia 21 kyr cal BP to present

Maps illustrate both pollen biome assignments and macrofossil occurrences through time. (Fig. 5; see Fig. S1 for the complete set of pollen-biome maps). At 21 kyr cal BP, treeless biomes dominate Eurasia. Most sites record either steppe (STEP; as defined either by Tarasov et al., 2000 or Bigelow et al., 2003) or dry tundra (DRYT, Bigelow et al., 2003, this biomization). Sites in northeast Siberia, along the north coast of Siberia and in Europe are dominated by forms of tundra, with DRYT the most common. Sites further south in central Asia are also STEP or DRYT. The Siberian lowlands have few data points, but, given the results of the topographic test, it is

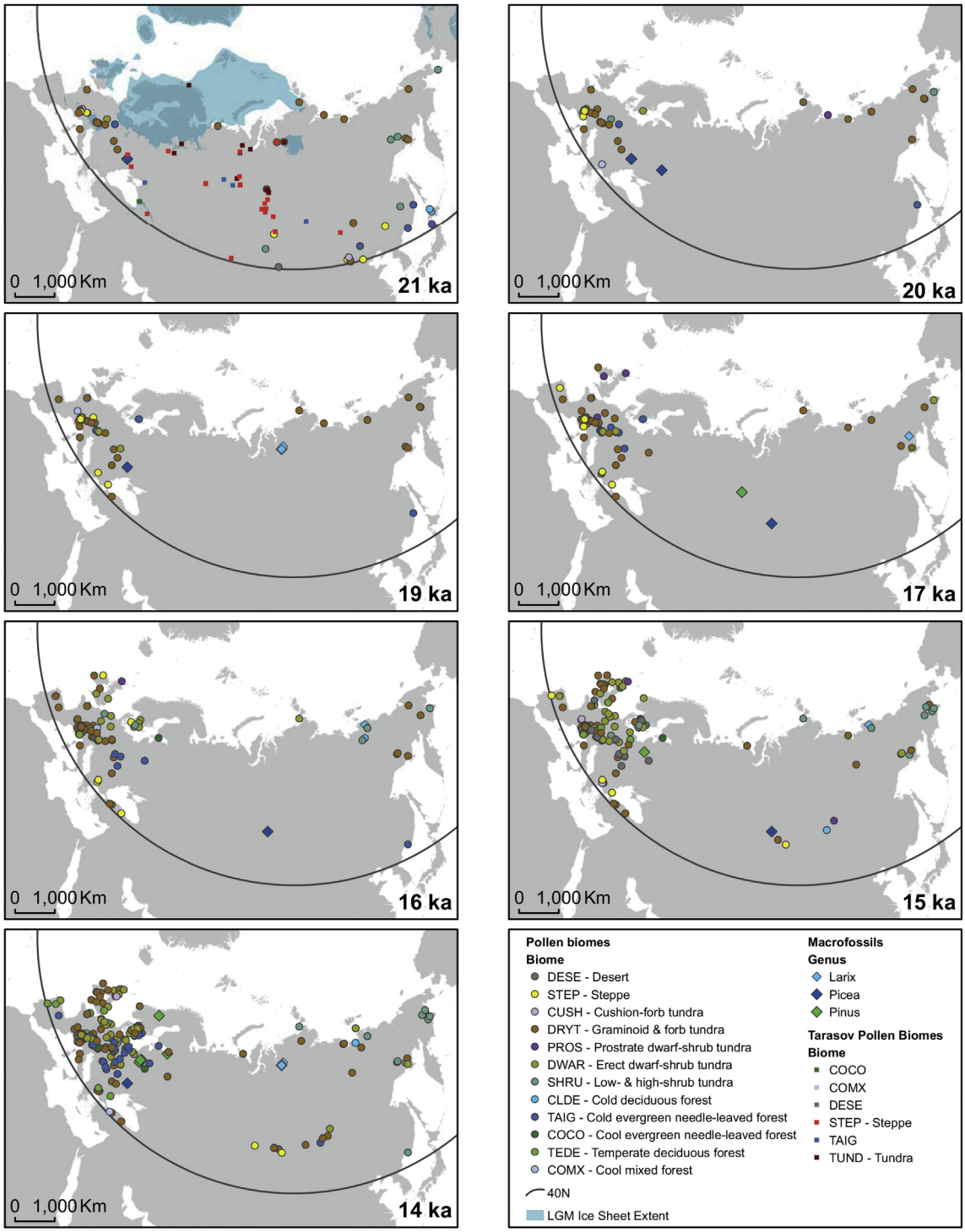

Fig. 5. a. Past vegetation biomes for key time slices for the whole study area from 21 to 14 kyr BP. Macrofossil occurrences are represented by diamonds. Squares on the 21 kyr BP map represent biomized sites from Tarasov et al. (2000). b. Past vegetation biomes for key time slices for the whole study area (left) and Europe only (right) from 13 ka to 9 kyr cal BP. Macrofossil occurrences are represented by diamonds. c. Past vegetation biomes for selected time slices for the whole study area (left) and Europe only (right) from 7 ka to 1 kyr cal BP. Macrofossil occurrences are represented by diamonds.

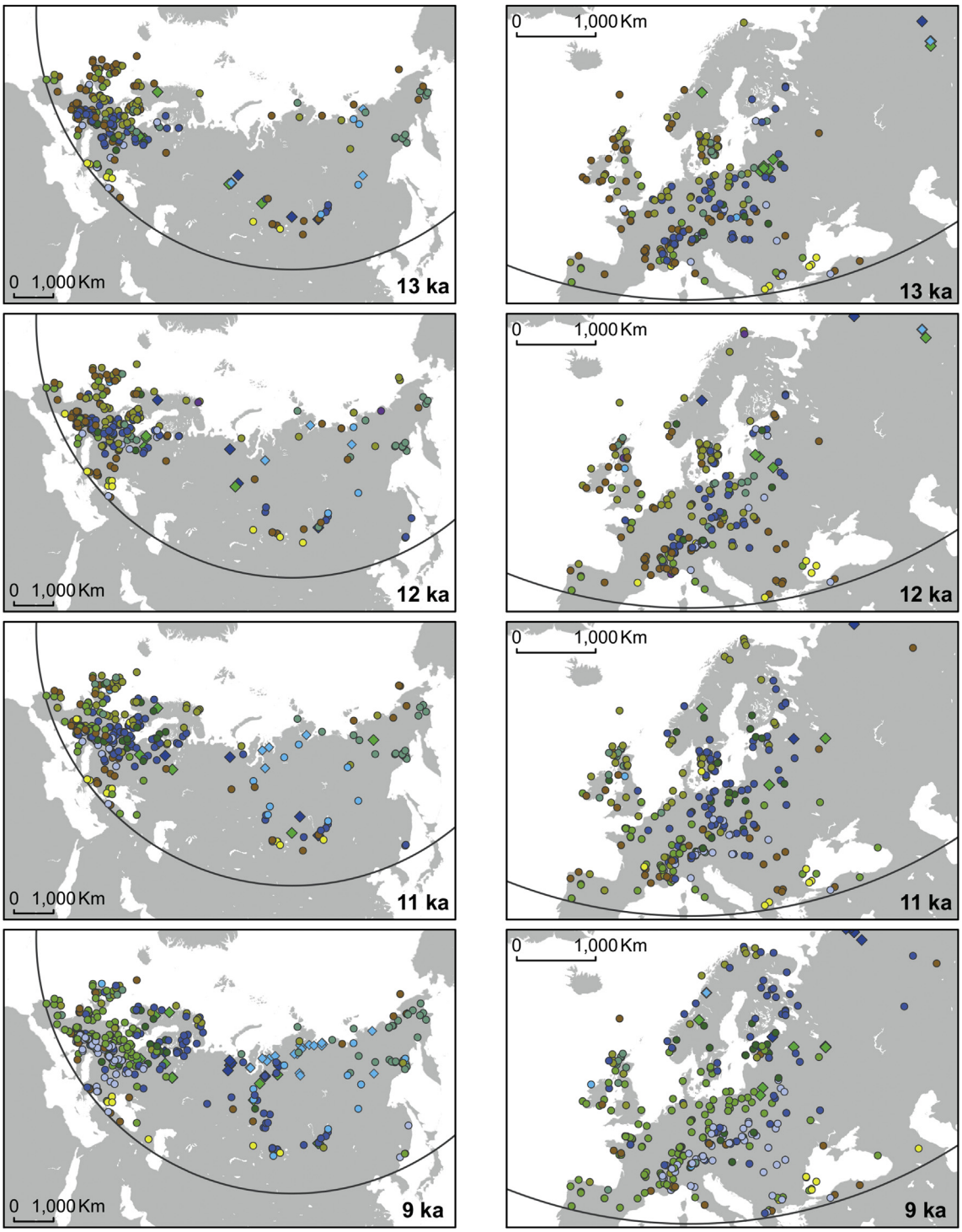

Fig. 5. (*continued*).

likely that tundra biomes would characterize much of this region. A few sites, however, record evergreen or deciduous coniferous forest (TAIG, CLDE), notably in the Caucasus and across mountainous central Asia to the Pacific Coast and Japan. In southern and central Europe, a few sites record forest biomes intermittently between 21 and 17 kyr BP. Subsequently, there is an increase in TAIG in southern and central Europe, and TAIG sites appear further east across the eastern European plain 16-15 ka. Eastward, tundra still dominates, but CLDE sites occur in both northeast and central Siberia from 15 kyr cal BP.

A major change is seen around 14 kyr cal BP. At this time, the number of palaeorecords increases markedly (Fig. 3). While DRYT is still common, in the far eastern region it tends to be replaced by low-high shrub tundra (SHRU). There is a continuing increase of TAIG, and temperate deciduous forest (TEDE) appears at some sites in southern and central Europe. The central Asian region remains steppe or DRYT. Some sites show CLDE in central and eastern Siberia.

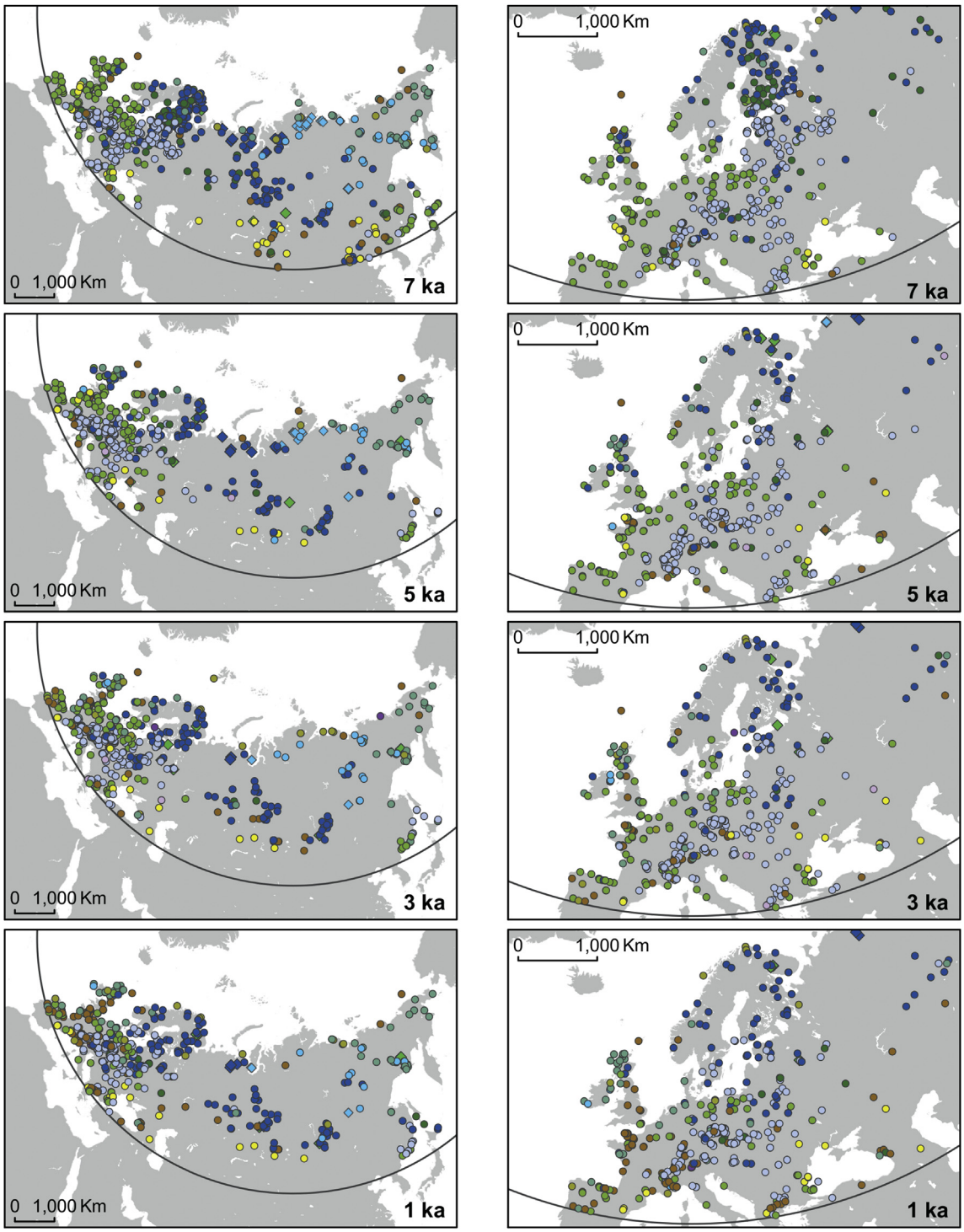

Fig. 5. (*continued*).

By 13 kyr cal BP, a mixture of DRYT and woody biomes characterizes the whole region, with TAIG and TEDE in the western region and TAIG and CLDE in the east. However, far eastern Siberia features a mixture of SHRU and DRYT. Treeless biomes are rare across Eurasia by 9 kyr cal BP. Of the forest biomes, TEDE dominates in Europe and TAIG and CLDE across Siberia. The Near East and central Asia still indicate STEP/DRYT along the southern margins of the study area. By 8 kyr cal BP, the arrangement of biomes approaches the modern pattern. The 7 kyr cal BP map includes data from the BIOME 6000 database, and these extra sites allow good demarcation of the steppe region across western and central Asia. Holocene treeline changes along the northern forest-tundra ecotone in central and eastern Siberia, where *Larix* forms the treeline, are clarified by the combination of the macrofossil record with the pollen biomes. In particular, a southward retreat from the Arctic Ocean coast after 5 kyr BP is discernible. From 2 to 0 kyr cal BP, DRYT increases noticeably in Europe.

4.4. Super PFTs

The percent summed PFT abundances, as recorded by the taxon scores (which are subject to square-root transformation) change with time (Fig. 6a and b). The observed patterns may partly reflect biased spatial sampling of the vegetation through time. For example, prior to 14 kyr BP, more southerly sites are an important geographic component, and the 21 kyr BP (eastern) value of 20% conifers reflects sites in China and Japan recording coniferous forest. While the fine details of changes are probably not significant, a few major patterns are worth considering. Across the whole region the main trend is that non-woody PFTs (grasses, sedges, forbs, including *Artemisia*) are dominant until 15 kyr cal BP. The square-root transformation favours the forb PFT, as nearly all forbs are underrepresented and have low pollen values. This feature highlights two effects: i) proportions of biomized forbs and graminoids, which constitute the herbaceous component of the vegetation, are approximately equal and ii) the proportion of herbaceous PFTs continuing into the Holocene is far greater than is typically interpreted from pollen diagrams. Between 15 and 8 kyr cal BP the non-

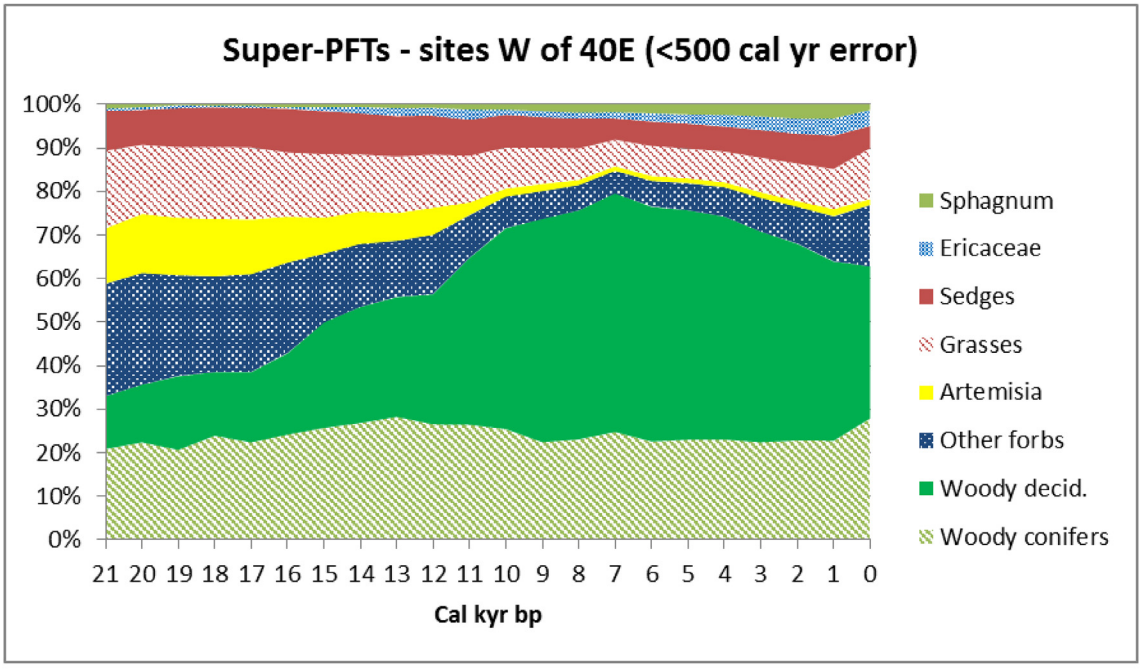

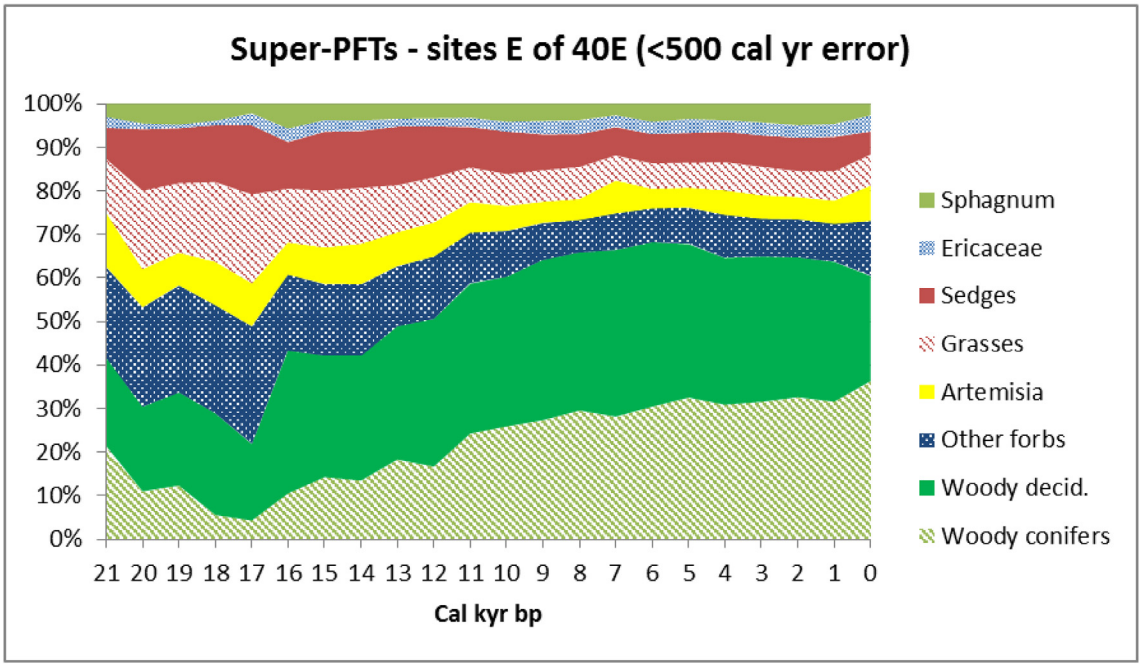

Fig. 6. Proportions of Super-PFTs across the 21 time slices. a) sites west of 40°E; b) sites east of 40°E.

woody PFTs are reduced and the deciduous woody PFT expands. The deciduous woody PFT includes *Betula, Alnus* and *Salix*, which can represent tundra shrubs as well as trees. Thus this increase may be interpreted as an expansion of forest growth forms or of tundra shrubs, depending upon region. In the Holocene, this PFT expands in the west considerably more, reflecting the greater importance of deciduous trees in western Eurasian forests, while the coniferous woody PFT expands in the east, reflecting the dominance of coniferous forest. Although Ericales and *Sphagnum* form a small proportion of all values, these PFTs, which are indicative of mesic and wetland conditions, increase beginning about 15 kyr cal BP and continue to increase until the present in the western region.

The plots of the percent tree and non-tree pollen biomes for time slices before, during and after the Younger Dryas stade (~12.9–11.7 kyr cal BP) are shown in Fig. 7. A drop in the abundance of woody biomes is clear at 12 ka. However, most of the signal is derived from the western sector (Fig. 7b); there is no clear pattern in the east.

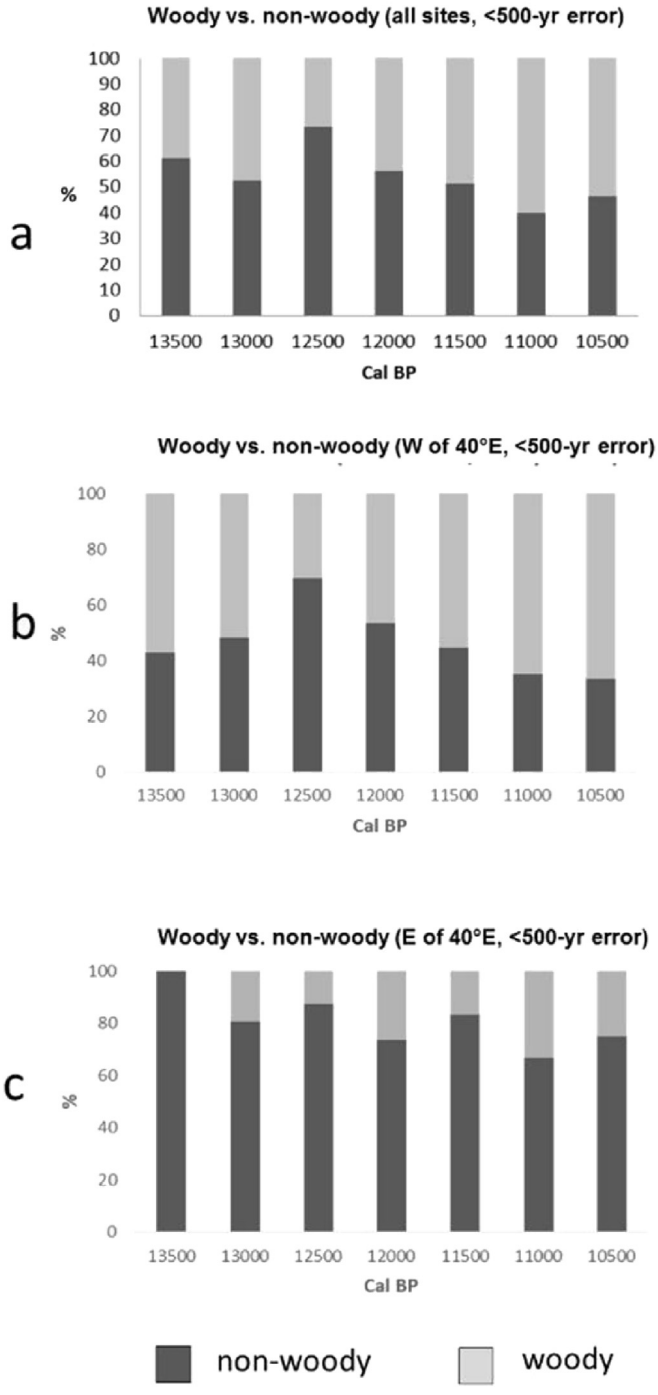

Fig. 7. Proportion of woody vs. non-woody biomes from 13,500 to 10,500 cal BP, derived from super-PFT sums; a – all sites, b – western sites, c – eastern sites.

5. Discussion

5.1. Modern pollen-vegetation comparison

When mapped in large numbers, the modern pollen data delineate major biomes and their ecotones relatively well (see Table 3). Error patterns are explainable by six factors that are not mutually exclusive: geographic proximity to other vegetation biomes; floristic similarity between pollen biomes; over-representation of woody vs non-woody taxa; the reliability of modern vegetation mapping; site type; and site density. The degree of geographic proximity refers to the location of the pollen site relative to areas of vegetation transition. For example, there is overlap of boreal pollen biomes to tundra vegetation. This is because the generally abundant pollen types *Pinus* (pine) and *Picea* (spruce) are key constituents of the pollen biome TAIG and tend also to occur in pollen spectra derived from adjacent shrub tundra. In the European mountains, TEDE and COMX pollen biomes are intermingled, probably because the pollen biomes differ by only a few key taxa and the vegetation mosaic has a relatively fine spatial scale. The degree of floristic similarity of pollen-based biomes determines how robust the assignments are in relation to small changes in pollen percentage values. This is particularly seen in the interchangeability of desert (DESE), STEP and DRYT, which share a large sub-set of taxa and are defined by forb or xeric shrub taxa that mainly have low pollen productivity. In fact, it is not possible to distinguish steppe from desert in our modern pollen data.

The tendency for woody taxa to produce relatively large quantities of pollen creates a bias that is not fully corrected by the square-root transformation, so typically forest biomes map on to non-forest areas such as tundra and steppe (see above). Where several biomes form a hierarchy of floristic subsets reflecting net primary productivity levels (e.g. the set of tundra biomes, or STEP and DESE), errors typically run in the direction of a more productive pollen biome being assigned to a less productive vegetation type, due to the pollen representation bias of woody taxa over most herbaceous taxa (in the case of tundra) or non-local pollen over virtually no local pollen (in the case of deserts). The exception is CLDE, which is characterized by *Larix*, a taxon with extremely low pollen representation. The evergreen coniferous pollen signal (TAIG) within the deciduous (*Larix*-dominated) conifer biome of eastern Siberia is likely due to the presence of *Pinus sibirica*, which occurs as far east as the Lena River and Lake Baikal and which has high pollen productivity. On the other hand, *Pinus pumila* is mostly restricted to the north-easternmost part of Asia and thus only contributes to the CLDE biome; here the CLDE is better represented. In the southeast coastal region, *P. koreana* likely contributes pollen to the forest biomes.

Mapping the modern land cover as potential natural vegetation may be an unrealistic approach in Europe and western Asia, where across large areas forest biomes have been replaced by agricultural land. Here there is a striking over-abundance of DRYT assignments, and, to a lesser extent, STEP. It is difficult to define an agricultural biome through pollen, as the indicators of cultivation are a suite of taxa with poor pollen representation (but see Fyfe et al., 2015; Trondman et al., 2015). DRYT and STEP are both defined by the

presence of grass (Poaceae), which is also a major component of agroecosystems, and it is not surprising that they appear across cultivated areas in these regions.

The examination of modern patterns has implications for interpreting the palaeorecords. Perhaps the clearest of these is site density. For older time slices, when sites are sparse, the modern analysis suggests that more reliance might be placed on extrapolating records across uniform topography (e.g., the Eurasian plains) than when interpreting palaeovegetation for topographically complex regions (i.e., mountain regions). A similar caution relates to ecotones, where biome assignment may be more ambiguous than for sites located more centrally within a biome. Furthermore, the occurrence of pollen of woody taxa in the record, assuming relative pollen productivity does not change over time, may bias results towards reconstructing a biome with more vegetation biomass than was actually present.

Ideally, site type should be considered when evaluating the regional applicability of an assigned biome. Bigelow et al. (2003) showed that lacustrine records reflect a more regional pollen signal and moss polsters a local signal. Siberian records derived from yedoma (icy silt deposits), thus basically from palaeosols, will tend to give a local signal. The dataset has incomplete metadata, meaning only a subset of sites can be typed. Of 5920 total site entities (including localities with multiple sections), 810 are lakes and 1717 are located in non-lake situations (e.g, moss polster, peat, yedoma); the remainder are undefined (Fig. 8).

5.2. Palaeovegetation record: past biomes

Biome maps and PFT trends clarify large-scale changes in biome distributions since the LGM, shifts in PFT dominance in space and time, and the temporal trends in establishment of forested biomes during deglaciation (Figs. 5–7).

The widespread dominance of DRYT, plus occurrences of steppe and other tundra types, indicates that the full-glacial landscape of Eurasia was largely treeless (see also Tarasov et al., 2000; Bigelow et al., 2003). Deglaciation and the accompanying major rearrangement of the climate system is reflected by dramatic changes in the dominant biomes, particularly the expansion of forest biomes and woody plant cover in general. The spread of forest biomes appears underway by 15 kyr cal BP in Europe and complete across the region by 13 kyr cal BP. Thus, the two millennia centred on 14 ka mark the critical transition from predominantly glacial to predominantly interglacial climate.

The marked increase in sites recording data between 15 and 13 kyr cal BP (centred on 14 kyr cal BP) is not an artefact of sample number and dating errors (see above). Both lakes and peatlands require enough moisture to exist, and the increase of sites at this time most likely represents a region-wide increase in effective moisture, probably largely driven by increased precipitation. Notably, the abundance of *Sphagnum* begins to increase at this time (there is also a later increase, in the early Holocene, particularly west of 40° E). As site coverage increases from 14 kyr cal BP, the northern edge of the steppe region of central Asia and the northern treeline become clear in the maps.

A moderate drop in woody PFTs occurs in Europe (W of 40° E) during the 12.5 kyr cal BP time slice (Fig. 7). This may reflect some retreat/thinning of forest cover during the Younger Dryas (YD) stade, which is expressed strongly in NW Europe but far more weakly with distance eastward from the Atlantic (Kokorowski et al., 2008). At 12 kyr cal BP and in subsequent time slices in central and eastern Siberia, CLDE sites are scattered across the region, suggesting an expansion of cold deciduous (*Larix*-dominated) forest at about this time. While the low number of sites in this region limits conclusions, there is no clear YD signal.

From 11 to 9 kyr cal BP TAIG in Europe retreats northwards and

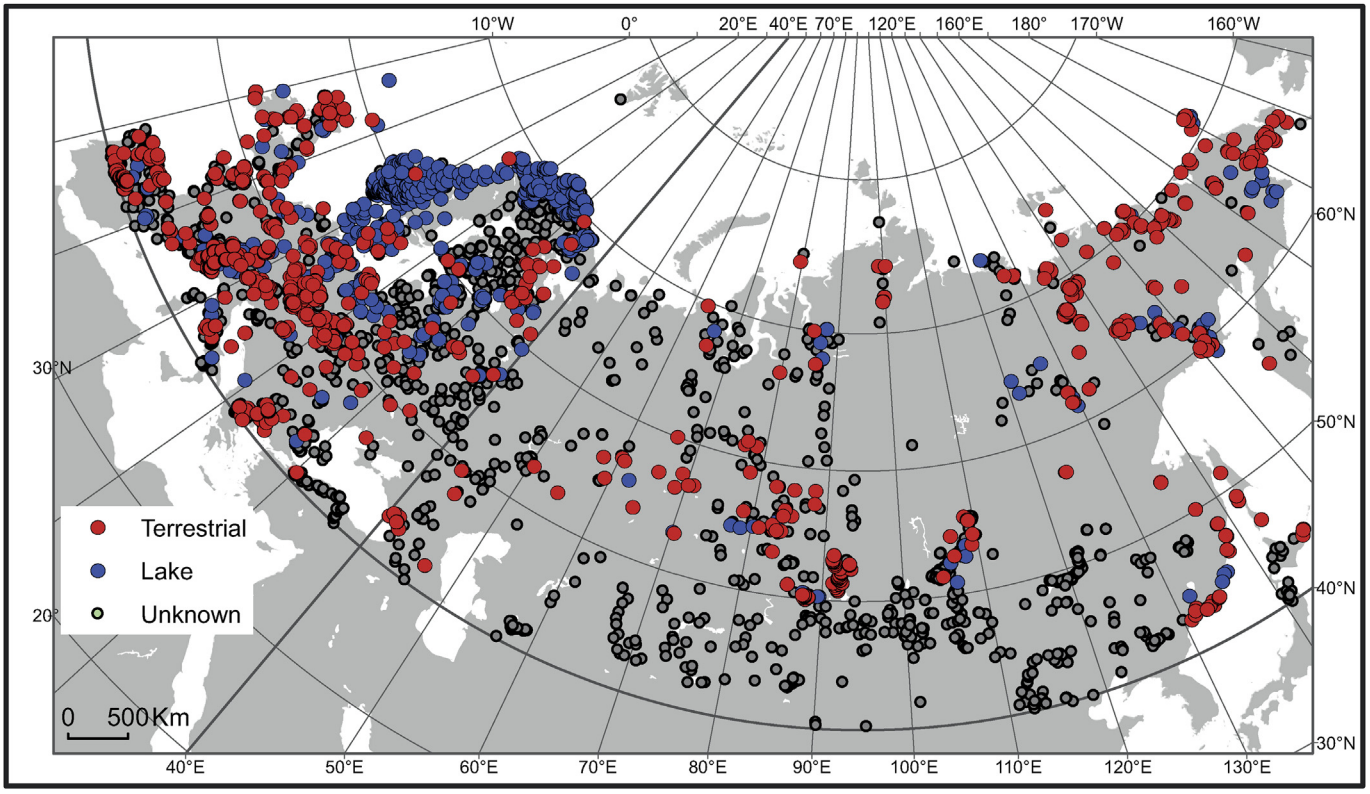

Fig. 8. Site-type distributions for the modern pollen dataset. The "unknown" category primarily affects surface samples.

COMX expands. This likely reflects the appearance of deciduous taxa at higher elevations and latitudes than before. The well-documented northern expansion of TEDE (Huntley, 1988; Prentice et al., 2000) 8–4 kyr cal BP is seen in Scandinavia. The northern treeline, represented by TAIG in the west and CLDE in the east, can be seen extending to the Arctic Ocean across much of Eurasia by 9000 kyr cal BP. There is a suggestion of treeline retreat in eastern and central Siberia between 5 and 3 kyr cal BP (see also Binney et al., 2009). From 3 kyr cal BP to present, DRYT - interpreted as a signal of open agricultural land - increases across Europe (see below).

5.3. Comparison with other simulated climate and vegetation data for the region

A major concern about current warming of the northern high latitudes is the extent to which woody vegetation (forest or shrub tundra) will expand at the expense of herbaceous tundra. So-called "arctic greening" has been widely reported (e.g., Sturm et al., 2001; Goetz et al., 2005; Forbes et al., 2010), and its consequences include modification of the land-surface feedback to climate (e.g., Chae et al., 2015). A similar change has been described as forest and shrub-tundra biomes replaced herbaceous biomes across northern Eurasia during deglaciation (Velichko, 2009). How well past woody vs herbaceous cover can be simulated based on palaeoclimate model output therefore has utility as regards future climate change and its potential impact on arctic vegetation.

The mapped fossil records can be compared with the vegetation modelling results of Allen et al. (2010), who used a DVGM (LPJ-guess) and a version of the general circulation model HadCM3 (Singarayer and Valdes, 2010) to estimate annual net primary productivity (aNPP) of different PFTs for Eurasia during the late Quaternary. From 21 kyr cal BP to 16 kyr cal BP, pollen biomes and PFTs are dominated by herbaceous taxa, while a few sites record TAIG or CLDE in Pacific Russia, Japan and Southern Europe. This mirrors the simulated pattern of high aNPP for mesophilous herbs from Eastern Europe to Chukotka (Allen et al., 2010). However, in Europe, boreal and summer green trees are simulated to have highest productivity. This pattern is not borne out by the pollen, which indicates DRYT and STEP dominated to the Atlantic coast at 21 kyr cal BP, suggesting the climate of Europe is simulated as warmer, or more likely moister, than it probably was.

After 21 kyr cal BP and until 16 kyr cal BP some pollen sites record forest biomes, particularly in coastal Asia and southern Europe, and, by 16 kyr cal BP, in the eastern European lowlands beyond the ice sheet. TEDE, COMX, and TAIG occur in Pacific coastal China and Russia and in Japan, TAIG and TEDE in Europe. At 14 kyr cal BP, the simulated boreal evergreen aNPP suggests conditions warm and moist enough to support tree growth in at least some locations, namely mountainous regions in southern Europe and in the north European plain; the pollen data support this. However, pollen data from mountainous central Asia indicate STEP and tundra biomes, whereas the simulation suggests boreal evergreen dominance. In this region of complex topography, the pollen data should be considered less reliable; however, the error is in the opposite direction from what might be expected (see section 3.3 above), which implies a mismatch between data and simulation. Scattered localities record CLDE in Siberia. The simulated data also suggest some tree growth may have been possible across Siberia, but the highest aNPP is still seen in mesophilous herbs. Thus both simulated and observed PFTs suggest largely open landscapes across the northeast at 14 kyr cal BP, but with trees present.

Finally, climate simulations for 7 kyr cal BP tend to show central Asia as dry, a feature related to strong evaporative land-surface feedback in models (Wohlfahrt et al., 2008). While the biome maps represent only the northern part of central Asia, there is little evidence of an expansion of dry-land biomes, which might be expected with heightened aridity.

5.4. Changes in land-surface properties

The abundances of the super-PFTs (Fig. 6) provide rough indications of trends in vegetation properties that reflect disturbance and/or biogeochemical processes. For example, while tundra and steppe do burn, boreal coniferous forest will have a greater effect on the occurrence of fires, associated changes in surface albedo and release of gaseous and particulate burn products to the atmosphere, as the fuel availability and burn severity in this biome is far greater than in the other biomes. In the eastern region, the conifer super PFT minimum values of <10% at 18-17 kyr cal BP gradually increase during deglaciation to reach ~30% by 9–8 ka, from which time the Siberian boreal forest likely contributed significantly to total global fires. The increases in *Sphagnum* and Ericales, beginning about 14 kyr cal BP and accelerating at the beginning of the Holocene, are an approximation of wetland initiation. Thus, they broadly mirror the importance of wetlands as a component of land cover across Eurasia and the potential for increased carbon sequestration and methanogenesis from the onset of the Holocene.

5.5. Implications for late-Pleistocene herbivore populations

The biomized PFT values indicate that traditional pollen-based interpretations probably under-estimate the contribution of forbs to the vegetation at 21 kyr cal BP and in subsequent millennia. For example, other forbs are equal in abundance to *Artemisia* (Fig. 6), and forb PFT values are similar to those of graminoids. This finding matches that of Willerslev et al. (2014), who proposed based on sedimentary DNA evidence, that forbs had an equal, if not dominant, role in full-glacial vegetation along with graminoids. Macrofossils (e.g., Kienast et al., 2005) also point to an important role for forb taxa in the full-glacial vegetation. The significance of this is yet to be fully investigated. While grasses were an important element of forage, relatively high diversity and biomass of forbs provides a variety of forage types and plant chemistry, broad options for self-medication (Forbey et al., 2009), and seasonal variation in availability of forage. This, along with actual primary productivity levels (Allen et al., 2010), may have contributed significantly to the carrying capacity of the vegetation that supported the megafauna.

The biome data show that from ~16 kyr cal BP, Europe supported a mosaic of woody and herbaceous vegetation. This persisted through the YD, with some fluctuations in proportional cover, until forest biomes became dominant at 10 kyr cal BP. In contrast, central and eastern regions featured predominantly treeless vegetation until 14-13 kyr cal BP. Thus, as suggested by Lister and Stuart (2008), different mammalian species were confronted with rather different vegetation configurations in the western and eastern regions, which in turn would have affected adaptation and survival of their populations through deglacial changes.

The change to forest and shrub-tundra biomes from herbaceous biomes across northern Eurasia during deglaciation has been linked with population reduction and eventual extinction of grazing herbivores (e.g., Stuart et al., 2004; Guthrie, 2006; MacDonald et al., 2012). Between 14 and 10 kyr cal BP, woody biomes, either SHRU or CLDE, gradually replaced DRYT in central and eastern Siberia, except along the northern coast, where DRYT persisted. This pattern supports the observation from radiocarbon-dated fossil data that populations of grazing mammals such as the woolly mammoth (*Mammuthus primigenius*) gradually retreated northwards during deglaciation so that by the onset of the Holocene, ca 11 kyr cal BP, populations were highly restricted in far-northern

areas. Notably, DRYT is recorded on Wrangel Island through the Holocene, the locality that supported the last Holocene Eurasian population of mammoths (Vartanyan et al., 1993; Lister and Stuart, 2008).

5.6. Refugial populations of forest trees

The biome data summarize a large number of spatially distributed pollen sites and clarify that forest biomes occurred, at least locally, in unglaciated northern regions from ~17 kyr cal BP onwards. Finds of macrofossils of *Picea* and *Larix* across Eurasia (Binney et al., 2009; Fig. 5) also support this conclusion. Whether these populations were present through the LGM is less clear. The vast northern Eurasian region is topographically complex enough to have featured a wide range of local climates, and it is likely that refugial populations persisted, even under the generally cool, dry conditions of the full glacial. Using simulations, Huntley et al. (2013) demonstrated that short-lived interstades that punctuated glacial conditions allowed for temporary expansion of tree populations. The temporal resolution of our data is such that the chances of pollen sites recording such localized (in time and space) tree population expansions are low. The reverse, a temporary contraction of tree cover, is shown in the Younger Dryas chronozone, as this period is within the temporal resolution of the data (Fig. 7). However, it should not be firmly concluded that putative refugial populations (observed or simulated) necessarily contributed extensively to local modern populations, as the spread of new individuals from adjacent regions and widespread gene exchange would have occurred over several millennia as climates rapidly changed (Semerikov et al., 2013; Edwards et al., 2014). Further study on the genetic impact of northern refugia on the development of modern forest populations is required.

5.7. Late-Holocene deforestation

The biome DRYT is characterized by grass and a range of plant families (Asteraceae, Brassicaceae, Caryophyllaceae, etc.) that are typical of temperate meadow communities as well as tundra. Thus DRYT appears as a common biome in Europe in the past two millennia, particularly at 1 kyr cal BP and in the modern dataset. Its distribution demarcates areas of Europe where deforestation was already widespread in medieval times and which are now intensive agricultural regions. The absence of the DRYT (or similar) option explains why in the northern continents, previous biomizations did not identify agricultural landscapes (e.g., Prentice et al., 2000). The issues of pollen representation that lead to the underestimation of open land in traditional pollen studies are summarized by Trondman et al. (2015), who apply a new algorithm (Sugita, 2007a) to pollen data in NW Europe and demonstrate that the proportion of open land at 3 kyr cal BP and within the most recent millennium are considerably greater than previously thought, which is in accordance with our biomization results. Similarly, Fyfe et al. (2015) combine PFTs into land-use groups, and by numerically emphasizing key agricultural indicator taxa, argue that open land is detectable as early as 6 ka. All these approaches, including the relatively straightforward biomization methodology used here, operate by modifying pollen values to reduce bias due to differential pollen productivity. All studies emphasize that the degree of deforestation in Europe has been greater than previously thought, particularly over the past 1000–2000 years.

6. Conclusions

This database analysis reflects both the strengths and weaknesses of large pollen datasets. Large-scale patterns in vegetation cover are usefully approximated by pollen data, and, at the continental scale, the resultant patterns can be used to assess critical changes in surface properties or compare with simulated vegetation data. However, error rates in assigning biomes, particularly in regions of complex topography, need to be borne in mind when interpreting past vegetation. For Eurasia, as far as incomplete metadata show, the majority of sites are terrestrial and thus are biased towards a local record. These limitations argue against creating land-cover estimates by interpolation of pollen data points alone. However, the large number of sites (more than mapped), which have been quality-checked, the associated error information, and the high level of floristic detail may make this database useful for a range of further analyses.

Acknowledgements

This work was funded by Natural Environment Research Council QUEST grant NE/D001578/ to ME and KW, and by grants 15-I-6-073 and 15-I-2-067 from the Russian Academy of Sciences and grant 15-05-06420 from the Russian Foundation for Fundamental Research, Far East Branch to AL. JOK was supported by the European Research Council (313797, COEVOLVE). Partial support for SK came from the Scientific Project of IGM SB RAS no. 0330-2016-0018 (Lab 284); this paper is a contribution to the Russian Foundation for Basic Research Project no. 15-05-00678 (SK). A Natural Environment Research Council Independent Research Fellowship (NE/L011859/1) funded M.M.-F.'s contribution. AA's contribution was partly sponsored by the Russian Government Program of Competitive Growth of Kazan Federal University. A data workshop in Southampton was funded by a supplement from the NERC-QUEST programme. A grant from IGBP-PAGES supported EB's and IK's travel. Some of the pollen data came from the European Pollen Database (EPD; http://www.europeanpollendatabase.net/), the NEOTOMA database (http://www.neotomadb.org/) and the BIOME 6000 database (https://www,ncdc.noaa.gov/paleo/biome6000.html), and we thank the data contributors and management groups for making these data available. The links to the databases can be found at 10.5285/6aeba247-52d1-4e84-949f-603742af40c1 (NERC) and http://eprints.soton.ac.uk/id/eprint/403426.

Appendix A. Supplementary data

Supplementary data related to this article can be found at http://dx.doi.org/10.1016/j.quascirev.2016.11.022.

References

Allen, J.R.M., Hickler, T., Singarayer, J.S., Sykes, M.T., Valdes, P.J., Huntley, B., 2010. Last glacial vegetation of northern Eurasia. Quat. Sci. Rev. 29, 2604–2618.

Anderson, P.M., Edwards, M.E., Brubaker, L.B., 2004. Results and paleoclimate implications of 35 years of paleoecological research in Alaska. In: Gillespie, A.E., Porter, S.C., Atwater, B.F. (Eds.), The Quaternary Period in the United States. Developments in Quaternary Science. Elsevier, New York, pp. 427–440.

Andreev, A., Tarasov, P., 2013. Northern Asia [postglacial pollen records]. In: Elias, S.A., Mock, C.J. (Eds.), Encyclopedia of Quaternary Science, second ed., vol. 4. Elsevier, Amsterdam, pp. 164–172.

Barnosky, A.D., Koch, P.L., Feranec, R.S., Wing, S.L., Shabel, A.B., 2004. Assessing the causes of late pleistocene extinctions on the continents. Science 306, 70–75.

Barr, I.D., Clark, C.D., 2012. Late Quaternary glaciations in Far NE Russia: combining moraines, topography and chronology to assess regional and global glaciation synchrony. Quat. Sci. Rev. 53, 72–87.

Bartlein, P.J., Harrison, S.P., Brewer, S., Connor, S., Davis, B.A.S., Gajewski, K., Guiot, J., Harrison-Prentice, T.I., Henderson, A., Peyron, O., Prentice, I.C., Scholze, M., Seppa, H., Shuman, B., Sugita, S., Thompson, R.S., Viau, A.E., Williams, J., Wu, H., 2011. Pollen-based continental climate reconstructions at 6 and 21 ka: a global synthesis. Clim. Dyn. 37, 775–802.

Bigelow, N.H., Brubaker, L.B., Edwards, M.E., Harrison, S.P., Prentice, I.C., Anderson, P.M., Andreev, A.A., Bartlein, P.J., Christiansen, T.R., Cramer, W., Kaplan, J.O., Lozhkin, A.V., Matveyeva, N.V., Murray, D.F., McGuire, A.D., Razzhivin, V.Y., Ritchie, J.C., Smith, B., Walker, D.A., Gajewski, K., Wolf, V.,

Holmqvist, B.H., Igarashi, Y., Kremenetskii, K., Paus, A., Pisaric, M.F.J., Volkova, V.S., 2003. Climate change and arctic ecosystems: 1. Vegetation changes north of 55 N between the last glacial maximum, mid-Holocene, and present. J. Geophys. Res. 108 (D19), 8170. http://dx.doi.org/10.1029/2002JD002558.

Binney, H.A., Willis, K.J., Edwards, M.E., Bhagwat, S.A., Anderson, P.M., Andreev, A.A., Blaauw, M., Damblon, F., Haesaerts, P., Kienast, F., Kremenetski, K.V., Krivonogov, S.K., Lozhkin, A.V., MacDonald, G.M., Novenko, P.O., Sapelko, T., Väliranta, M., Vazhenina, L., 2009. The distribution of late-Quaternary woody taxa in northern Eurasia: evidence from a new macrofossil database. Quat. Sci. Rev. 28, 2445–2464. http://dx.doi.org/10.1016/j.quascirev.2009.04.016.

Binney, H.A., Gething, P.W., Nield, J.M., Sugita, S., Edwards, M.E., 2011. Treeline identification from pollen data: beyond the limit? J. Biogeogr. 38, 1792–1806.

Birks, H.J.B., Willis, K.J., 2008. Alpines, trees, and refugia in Europe. Plant Ecol. Divers. 1, 147–160. http://dx.doi.org/10.1080/17550870802349146.

Blaauw, M., 2010. Methods and code for 'classical' age-modelling of radiocarbon sequences. Quat. Geochronol. 5, 512–518.

Campos, P.F., Willerslev, E., Sher, A., Orlando, L., Axelsson, E., Tikhonov, Aaris-Sorensen, K., Greenwood, A.D., Kahlke, R.D., Kosintsev, P., Krakhmalnaya, T., Kuznetsova, T., Lemey, P., MacPhee, R., Norris, C.A., Shepherd, K., Suchard, M.A., Zazula, G.D., Shapiro, B., Gilbert, M.T.P., 2010. Ancient DNA analyses exclude humans as the driving force behind late Pleistocene musk ox (Ovibos moschatus) population dynamics. PNAS 107, 5675–5680.

Chae, Y., Kang, S.M., Jeong, S.J., Kim, B., Frierson, D.M.W., 2015. Arctic greening can cause earlier seasonality of Arctic amplification. Geophys. Res. Lett. 42536–42541. http://dx.doi.org/10.1002/2014GL061841.

Edwards, M.E., Armbruster, W.S., Elias, S.E., 2014. Constraints on post-glacial boreal tree expansion out of far-northern refugia. Global Eco. Biogeogr. 23, 1198–1208.

Forbes, B.C., Fauria, M.M., Zetterberg, P., 2010. Russian Arctic warming and 'greening' are closely tracked by tundra shrub willows. Glob. Change Biol. 16, 1542–1554.

Forbey, J.S., Harvey, A.L., Huffman, M.A., Provenza, F.D., Sullivan, R., Tasdemir, D., 2009. Exploitation of secondary metabolites by animals: a response to homeostatic challenges. Integr. Comp. Biol. 49, 314–328.

Fyfe, R.M., Woodbridge, J., Roberts, N., 2015. From forest to farmland: pollen-inferred land cover change across Europe using the pseudobiomization approach. Glob. Change Biol. 21, 1197–1212. http://dx.doi.org/10.1111/gcb.12776.

Gaillard, M.-J., Sugita, S., Bunting, J., Dearing, J., Bittmann, F., 2008. Human impact on terrestrial ecosystems, pollen calibration and quantitative reconstruction of past land cover. Veg. Hist. Archaeobot. 17, 415–418.

Goetz, S.J., Bunn, A.G., Fiske, G.J., Houghton, R.A., 2005. Satellite-observed photosynthetic trends across boreal North America associated with climate and fire disturbance. PNAS 102, 13521–13525.

Guthrie, R.D., 1990. Frozen Fauna of the Mammoth Steppe. University of Chicago Press, Chicago.

Guthrie, R.D., 2006. New carbon dates link climatic change with human colonization and Pleistocene extinctions. Nature 441, 207–209.

Hoogakker, B.A.A., Smith, R.S., Singarayer, J.S., Marchant, R., Prentice, I.C., Allen, J.R.M., Anderson, R.S., Bhagwat, S.A., Behling, H., Borisova, O., Bush, M., Correa-Metrio, A., de Vernal, A., Finch, J.M., Fréchette, B., Lozano-Garcia, S., Gosling, W.D., Granoszewski, W., Grimm, E.C., Grüger, E., Hanselman, J., Harrison, S.P., Hill, T.R., Huntley, B., Jiménez-Moreno, G., Kershaw, P., Ledru, M.-P., Magri, D., McKenzie, M., Müller, U., Nakagawa, T., Novenko, E., Penny, D., Sadori, L., Scott, L., Stevenson, J., Valdes, P.J., Vandergoes, M., Velichko, A., Whitlock, C., Tzedakis, C., 2016. Terrestrial biosphere changes over the last 120 kyr. Clim. Past 12, 51–73. http://dx.doi.org/10.5194/cp-12-51-2016.

Huntley, B., 1988. Europe. In: Huntley, B., Webb III, T. (Eds.), Vegetation History. Kluwer Academic Publishers, Dordrecht, pp. 341–383.

Huntley, B., Allen, J.R.M., Collingham, Y.C., Hickler, T., Lister, A.M., Singarayer, J., Stuart, A.J., Sykes, M.T., Valdes, P.J., 2013. Millennial climatic fluctuations are key to the structure of Last Glacial ecosystems. PLoS One 8, e69163.

Kaplan, J.O., Prentice, I.C., Buchmann, N., 2002. The stable carbon isotope composition of the terrestrial biosphere: modeling at scales from the leaf to the globe. Glob. Biogeochem. Cycles 16 (4). http://dx.doi.org/10.1029/2001GB001403. Article Number 1060.

Kaplan, J.O., Bigelow, N.H., Prentice, I.C., Harrison, S.P., Bartlein, P.J., Christensen, T.R., Cramer, W., Matveyeva, N.V., McGuire, A.D., Murray, D.F., Razzhivin, V.Y., Smith, B., Walker, D.A., Anderson, P.M., Andreev, A.A., Brubaker, L.B., Edwards, M.E., Lozhkin, A.V., 2003. Climate change and Arctic ecosystems: 2. Modeling, paleodata-model comparisons, and future projections. J. Geophys. Res. 108 (D19), 8171. http://dx.doi.org/10.1029/2002JD002559.

Kaplan, J.O., Krumhardt, K.M., Zimmermann, N., 2009. The prehistoric and preindustrial deforestation of Europe. Quat. Sci. Rev. 28, 3016–3034.

Kienast, F., Schirrmeister, L., Siegert, C., Tarasov, P., 2005. Palaeobotanical evidence for warm summers in the East Siberian Arctic during the last cold stage. Quat. Res. 63, 283–300.

Kokorowski, H.D., Anderson, P.M., Mock, C.J., Lozhkin, A.V., 2008. A re-evaluation and spatial analysis of evidence for a Younger Dryas climatic reversal in Beringia. Quat. Sci. Rev. 27, 1710–1722.

Liu, Z., Otto-Bliesner, B.L., He, F., Brady, E.C., Tomas, R., Clark, P.U., Carlson, A.E., Lynch-Stieglitz, J., Curry, W., Brook, E., Erickson, D., Jacob, R., Kutzbach, J., Cheng, J., 2009. Transient simulation of last deglaciation with a new mechanism for Bolling-Allerod warming. Science 325, 310–314.

Lister, A.M., Stuart, A.J., 2008. The impact of climate change on large mammal distribution and extinction: Evidence from the last glacial/interglacial transition. Comptes Rendues Geosci. 340, 615–620.

Lowe, J.J., Rasmussen, S.O., Björck, S., Hoek, W.Z., Steffensen, J.P., Walker, M.J.C., Yu, Z.C., the INTIMATE Group, 2008. Synchronisation of palaeoenvironmental events in the North Atlantic region during the Last Termination: a revised protocol recommended by the INTIMATE group. Quat. Sci. Rev. 27, 6–17.

Lozhkin, A.V., Anderson, P.M., 2013. Northern Asia [Late Pleistocene pollen records]. In: Elias, S.A., Mock, C.J. (Eds.), Encyclopedia of Quaternary Science, second ed., vol. 4. Elsevier, Amsterdam, pp. 27–38.

Lozhkin, A.V., Anderson, P.M., Vazhenina, L.N., 2011. Younger Dryas and early Holocene peats from northern Far East Russia. Quat. Int. 237, 54–64.

MacDonald, G.M., Beilman, D.W., Kuzmin, Y.V., Orlova, L.A., Kremenetski, K.V., Shapiro, B., Wayne, R.K., Van Valkenburgh, B., 2012. Pattern of extinction of the woolly mammoth in Beringia. Nat. Commun. 3, 893. http://dx.doi.org/10.1038/ncomms1881.

McLauchlan, K.K., Williams, J.J., Craine, J.M., Jeffers, E.S., 2013. Changes in global nitrogen cycling during the Holocene epoch. Nature 495, 352–355.

Pielke, R.A., Vidale, P.L., 1995. The boreal forest and the polar front. J. Geophys. Res. 100, 25755–25758.

Pitulko, V.V., Nikolsky, P.A., Girya, E.Y., Basilyan, A.E., Tumskoy, V.E., Koulakov, S.A., Astakhov, S.N., Pavlova, E.Y., Anisimov, M.A., 2004. The Yana RHS site: humans in the arctic before the Last Glacial maximum. Science 303, 52–56.

Prentice, I.C., Webb III, T., 1998. BIOME 6000: reconstructing global mid-Holocene vegetation patterns from palaeoecological records. J. Biogeogr. 25, 997–1005.

Prentice, I.C., Guiot, J., Huntley, B., Jolly, D., Cheddadi, R., 1996. Reconstructing biomes from palaeoecological data: a general method and its application to European pollen data at 0 and 6 ka. Clim. Dyn. 12, 185–194.

Prentice, I.C., Jolly, D., BIOME 6000 participants, 2000. Mid-Holocene and glacial-maximum vegetation geography of the northern continents and Africa. J. Biogeogr. 27, 507–519.

Rasmussen, S.O., Andersen, K.K., Svensson, A.M., Steffensen, J.P., Vinther, B.M., Clausen, H.B., Siggaard-Andersen, M.-L., Larsen, L.B., Dahl-Jensen, D., Bigler, M., Rothlisberger, R., Fischer, H., Goto-Azuma, K., Hansson, M.E., Ruth, U., 2006. A new Greenland ice core chronology for the last glacial termination. J. Geophys. Res. 111, D6102. http://dx.doi.org/10.1029/2005JD006079.

Reimer, P.J., Baillie, M.G.L., Bard, E., Bayliss, A., Beck, J.W., Bertrand, C., Blackwell, P.G., Buck, C.E., Burr, G., Cutler, K.B., Damon, P.E., Edwards, R.L., Fairbanks, R.G., Friedrich, M., Guilderson, T.P., Hughen, K.A., Kromer, B., McCormac, F.G., Manning, S., Bronk Ramsey, C., Reimer, R.W., Remmele, S., Southon, J.R., Stuiver, M., Talamo, S., Taylor, F.W., van der Plicht, J., Weyhenmeyer, C.E., 2004. IntCal04 Terrestrial radiocarbon age calibration, 26-0 ka BP. Radiocarbon 46, 1029–1058.

Semerikov, V.L., Semerikova, S.A., Polezhaeva, M.A., Kosintsev, P.A., Lascoux, M., 2013. Southern montane populations did not contribute to the recolonization of West Siberian Plain by Siberian larch (*Larix sibirica*): a range-wide analysis of cytoplasmic markers. Mol. Ecol. 22, 4958–4971.

Serreze, M.C., Barry, R.G., 2011. Processes and impacts of Arctic amplification: a research synthesis. Glob. Planet. Change 77, 85–96.

Sher, A.V., 1997. Late-Quaternary extinction of large mammals in northern Eurasia: a new look at the Siberian contribution. In: Huntley, B., Cramer, W., Morgan, A.V., Prentice, H.C., Allen, J.R.M. (Eds.), Past and Future Rapid Environmental Changes: the Spatial and Evolutionary Responses of Terrestrial Biota. Springer-Verlag, Berlin-Heidelberg-New York, pp. 319–339.

Singarayer, J.S., Valdes, J.S., 2010. High-latitude climate sensitivity to ice-sheet forcing over the last 120 kyr. Quat. Sci. Rev. 29, 43–55.

Smith, L.C., MacDonald, G.M., Velichko, A.A., Beilman, D.W., Borisova, O.K., Frey, K.E., Kremenetski, K.V., Sheng, Y., 2004. Siberian peatlands a net carbon sink and global methane source since the early Holocene. Science 303, 353–356.

Stewart, J.R., Lister, A.M., 2001. Cryptic northern refugia and the origins of the modern biota. Trends Ecol. Evol. 16, 608–613.

Stuart, A.J., Kosintsev, P.A., Higham, T.F.G., Lister, A.M., 2004. Pleistocene to Holocene extinction dynamics in giant deer and woolly mammoth. Nature 431, 684–689.

Sturm, M., Racine, C., Tape, K., 2001. Increasing shrub abundance in the Arctic. Nature 411, 546–547.

Sugita, S., 2007a. Theory of quantitative reconstruction of vegetation I: pollen from large sites REVEALS regional vegetation composition. Holocene 17, 229–241.

Sugita, S., 2007b. Theory of quantitative reconstruction of vegetation II: all you need is LOVE. Holocene 17, 243–257.

Svendsen, J.I., Alexanderson, H., Astakhov, V.I., Demidov, I., Dowdeswell, J.A., Funder, S., Gataullin, V., Henriksen, M., Hjort, C., Houmark-Nielsen, M., Hubberten, H.W., Ingolfsson, O., Jakobsson, M., Kjaer, K.H., Larsen, E., Lokrantz, H., Lunkka, J.P., Lysa, A., Mangerud, J., Matiouchkov, A., Murray, A., Moller, P., Niessen, F., O.Nikolskaya, O., Polyak, L., Saarnisto, M., Siegert, C., Siegert, M.J., Spielhagen, R.F., Stein, R., 2004. Late quaternary ice sheet history of northern Eurasia. Quat. Sci. Rev. 23, 1229–1271.

Tarasov, P.E., Webb III, T., Andreev, A.A., Afanas'eva, N.B., Berezina, N.A., Bezusko, L.G., Blyakhararchuk, T.A., Bolikhovskaya, N.S., Cheddadi, R., Chernavskaya, M.M., Chernova, G.M., Dorofeyuk, N.I., Dirksen, V.G., Elina, G.A., Filimonova, L.V., Glebov, F.Z., Guiot, J., Gunova, V.S., Harrison, S.P., Jolly, D., Khomutova, V.I., Kvavadze, E.V., Osipova, I.M., Panova, N.K., Prentice, I.C., Saarse, L., Sevastyanov, D.V., Volkova, V.S., Zernitskaya, V.K., 1998. Present-day and mid-Holocene biomes reconstructed from pollen and plant macrofossil data from the former Soviet Union and Mongolia. J. Biogeogr. 25, 1029–1053.

Tarasov, P.E., Volkova, V.S., Webb, T., Guiot, J., Andreev, A.A., Bezusko, L.G., Bykova, G.V., Dorofeyuk, N.I., Kvavadze, E.V., Osipova, I.M., Panova, N.K., Sevastyanov, D.V., 2000. Last glacial maximum biomes reconstructed from

pollen and plant macrofossil data from northern Eurasia. J. Biogeogr. 27, 609–620.
Tarasov, P.E., Andreev, A.A., Anderson, P.M., Lozhkin, A.V., Haltia-Hovi, E., Nowaczyk, N.R., Wennrich, V., Brigham-Grette, J., Melles, M., 2013. A pollen-based biome reconstruction over the last 3.562 million years in the Far East Russian Arctic – new insights on climate-vegetation relationships at the regional scale. Clim. Past 9, 2759–2775.
Thompson, C., Beringer, J., Chapin, F.S., McGuire, A.D., 2004. Structural complexity and land-surface energy exchange along a gradient from arctic tundra to boreal forest. J. Veg. Sci. 15, 397–406.
Trondman, A.-K., Gaillard, M.-J., Mazier, F., Sugit, S., Fyfe, R., Nielsen, A.B., Twiddle, C., Barratt, P., Birks, H.J.B., Bjune, A.E., Björkman, L., Broström, A., Casledine, C., David, R., Dodson, J., Dörfler, W., Fischer, E., van Geel, B., Giesecke, T., Hultberg, T., Kalnina, L., Kangur, M., van der Knapp, P., Koff, T., Kuneš, P., Lagerås, P., Latalowa, M., Lechterbeck, J., Leroyer, C., Leydet, M., Lindblah, M., Marquer, L., Mitchell, F.J.G., Odgaard, B.V., Peglar, S.M., Persson, T., Poska, A., Rösch, M., Seppä, H., Veski, S., Wick, L., 2015. Pollen-based quantitative reconstructions of Holocene regional vegetation cover (plant-functional types and land-cover types) in Europe suitable for climate modelling. Glob. Change Biol. 21, 676–697.
Vartanyan, S.L., Garutt, V.E., Sher, A.V., 1993. Holocene dwarf mammoths from Wrangel island in the Siberian Arctic. Nature 362, 337–340.
Velichko, A.A. (Ed.), 2009. Paleoclimates and Paleoenvironments of Extra-tropical Regions of the Northern Hemisphere. Late Pleistocene-Holocene. GEOS, Moscow.
Velichko, A.A., Faustova, M.A., 2009. Glaciation during the late Pleistocene. In: Velichko, A.A. (Ed.), Paleoclimates and Paleoenvironments of Extra-tropical Area of the Northern Hemisphere Late Pleistocene-Holocene. Institute of Geography, Russian Academy of Sciences, Moscow, pp. 32–41.
Walter, K.M., Edwards, M.E., Grosse, G., Zimov, S.A., Chapin III, F.S., 2007. Thermokarst Lakes as a source of atmospheric CH_4 during the last deglaciation. Science 318, 633–636.
Willerslev, E., Davison, J., Moora, M., Zobel, M., Coissac, E., Edwards, M.E., Lorenzen, E.D., Vestergård, M., Gussarova, G., Haile, J., Craine, J., Bergmann, G., Gielly, L., Boessenkool, S., Epp, L.S., Pearman, P.B., Cheddadi, R., Murray, D., Bråthen, K.A., Yoccoz, N., Binney, H., Cruaud, C., Wincker, P., Goslar, T., Alsos, I.G., Bellemain, E., Brysting, A.K., Elven, R., Sønstebø, J.H., Murton, J., Sher, A., Rasmussen, M., Rønn, R., Mourier, T., Cooper, A., Austin, J., Möller, P., Froese, D., Zazula, G., Pompanon, F., Rioux, D., Niderkorn, V., Tikhonov, A., Savvinov, G., Roberts, R.G., MacPhee, R.D.E., Gilbert, M.P.T., Kjær, K., Orlando, L., Brochmann, C., Taberle, P., 2014. Fifty thousand years of arctic vegetation and megafauna diet. Nature 506, 47–51.
Williams, J.W., Tarasov, P., Brewer, S., Notaro, M., 2011. Late Quaternary variations in tree cover at the northern forest-tundra ecotone. J. Geophys. Res. 116, G01017. http://dx.doi.org/10.1029/2010JG001458.
Wohlfahrt, J., Harrison, S.P., Braconnot, P., Hewitt, C.D., Kitoh, A., Mikolajewicz, U., Otto-Bliesner, B.L., Weber, S.L., 2008. Evaluation of coupled ocean–atmosphere simulations of the mid-Holocene using palaeovegetation data from the northern hemisphere extratropics. Clim. Dyn. 31, 871–890.
Zimov, S.A., 2005. Pleistocene park: return of the Mammoth's ecosystem. Global voices of science: essays on science and Society. Science 308, 796–798.
Zimov, S.A., Chuprynin, V.I., Oreshko, A.P., Chapin, F.S., Reynolds, J.F., Chapin, M.C., 1995. Steppe-tundra transition - a herbivore-driven biome shift at the end of the Pleistocene. Am. Nat. 146, 765–794.
Zimov, S.A., Schuur, E.A.G., Chapin, F.S., 2006. Permafrost and the global carbon budget. Science 312, 1612–1613.